

Photoinduced chemical crosslinking activity and photo-oxidative stability of amine acrylates: photochemical and spectroscopic study

Norman S. Allen^{a,*}, Michaela C. Marin^a, Michele Edge^a, Derek W. Davies^b,
John Garrett^b, Frank Jones^b

^a*Department of Chemistry and Materials, The Manchester Metropolitan University, John Dalton Building, Chester Street, Manchester M1 5GD, UK*

^b*Akcros Chemicals, Eccles Site, Bentcliffe Way, PO Box 1, Eccles, Manchester M30 0BH, UK*

Received 17 January 2001; accepted 20 February 2001

Abstract

A number of dialkyl and heterocyclic amine-terminated diacrylate resins were prepared by a Michael addition reaction of the appropriate secondary amine with a triacrylate diluent monomer. Photocuring rates are found to be dependent upon the extent of UV absorption of the photoinitiator used with ITX in this case exhibiting the most rapid cure. There is no consistency in cure rate with amine structure. Transient absorption spectra on conventional microsecond flash photolysis are assigned to the formation of free radical intermediates by electron transfer. Photoinduced polymerisation activities of the resins measured by real-time infrared spectroscopy appear to be closely related to the formation of such transient species. The initiator structure is the more determining factor. Their photo-oxidative stability and photoyellowing (by UV derivative absorption) are studied after UV and electron-beam curing through Fourier transform infra-red (FTIR) and second derivative UV spectroscopic methods and hydroperoxide analysis. On photo-oxidation UV cured diluent monomer undergoes oxidation at a higher rate than EB cured systems. Initial photo-oxidation of the coatings as measured by hydroperoxide analysis and hydroxyl index via FTIR analysis exhibited similar changes. Again the oxidation profiles are dependent upon the terminal amine structure with 1-methylpiperazine exhibiting the strongest oxidation. Hydroxyl index showed generally an initial rise followed by a sharp decline and then a slow increase over much longer irradiation periods. The presence of the amine functionality is found to be an effective scavenger of oxygen and hydroperoxide formation in EB cured coatings. In the UV cured coatings the hydroperoxide levels are found generally to be significantly higher than in EB systems due to the photosensitising effect of the residual photoinitiator. Diluent monomer terminated with dialkylamine groups are found to be more prone to oxidation and UV absorption increase than alkanolamines, cycloaliphatic amines and heterocyclic amines. UV cured resins exhibit a more facile transient photoyellowing than the same electron-beam cured systems, and this is associated with hydrogen-atom abstraction and oxidation of the alkylamine group by the residual photoinitiator enhancing the rate of hydroperoxidation of the amine group. © 2001 Elsevier Science Ltd. All rights reserved.

Keywords: Photochemistry; Photopolymerisation; Photocuring; Photoinitiators; Amine acrylates; Hydroperoxides; Yellowing; Photooxidation

1. Introduction

There have been a number of investigations into the effect of photodegradation and photo-oxidation on the physical properties of radiation cured coatings [1–15]. The results have allowed an empirical relationship to be drawn between resin structure and degradation resistance. During the weatherometer ageing of EB cured

and UV cured coatings it was found that EB cured epoxy acrylates were less stable than their UV cured counterparts as indicated by film failure [4,5]. The same relationship was found, with respect to curing conditions, with a urethane acrylate. Other workers carried out a mechanistic and kinetic study of the photodegradation of a UV cured epoxy acrylate coating [7]. The epoxy diacrylate used was derived from the glycidyl ether of bisphenol-A and was studied in conjunction with tripropylene glycol diacrylate as a reactive diluent and benzil dimethyl ketal as photoinitiator. Because of no definitive changes in the pendulum hardness after an

* Corresponding author. Tel.: +44-161-247-1432; fax: +44-161-247-6357.

E-mail address: n.allen@mmu.ac.uk (N.S. Allen).

exposure time of 1000 h, they concluded that the reason for the high stability is due to the high crosslink density of the UV cured coatings. They observed also that on photoageing with wavelengths >250 nm the epoxy-acrylate coatings suffered important chemical modifications after only 140 h of irradiation. But under a N_2 atmosphere the coatings were much more resistant to UV degradation. They concluded that 80% of the functional group loss under air was due to oxidation reactions. On the other hand spectroscopic investigations have shown that EB cured coatings are generally more photostable than UV cured coatings [8–15]. Also, where the presence of free or bound amine functionality was present, as a cosynergist, the photostability was significantly improved. This was associated with the presence of the amine effectively scavenging oxygen via alkylamino radicals and thereby protecting the resin structure from hydroperoxidation. In this way, rates of hydroperoxidation were found to be markedly accelerated by the presence of residual UV initiators while in EB cured systems the rate was very low [9]. It was also found that residual hydrogen atom abstracting photoinitiators were more detrimental than photofragmenting photoinitiators in post-cured UV cured resin stability [8]. Discolouration of the cured coatings was also important and found to be highly dependent upon the structure of the amine co-synergist. Here the cured coatings were found to develop a high energy absorption band in the near UV region at 275 nm that was consistent with the growth and decay of the initial photoyellowing process encountered with radiation cured amine acrylate systems [12–15]. In relation to amine structure dialkylamines were found to photoyellow more than alkanolamines and in turn these yellowed more than cycloaliphatic amines such as dicyclohexylamine. This work was essentially based on the use and co-reaction of a diluent monomer TMPTA (trimethylolpropane triacrylate) via a Michael addition reaction. In this work we have extended the study to another type of acrylated diluent monomer Actilane 430 (acrylated trimethylolpropane ethoxylate) where the influence of ether substitution could be important in the post-cured photoreactions. Here a range of secondary amines have been utilised and extended via the Michael addition reaction to cover an intercomparison of dialkylamines, alkanolamines and heterocyclic amines. In the previous work the length of the alkyl chain was found to be important in terms of controlling the extent of photoyellowing and therefore, a long chain amine has been included based on coco-amine. Photo-oxidative stabilities of the post-cured resins have been evaluated via hydroperoxide analysis, FTIR and UV second derivative spectroscopy. The influence of amine structure on cure rates has also been undertaken using real-time infra-red analysis (RTIR) since this could have an important bearing on post-cured properties.

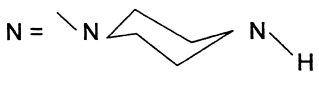

2. Experimental

2.1. Materials

The solvents used were spectroscopic or HPLC grade quality and were supplied by the Sigma-Aldrich Company Limited, UK, including also the compounds used in the synthetic procedures. The benzophenone and ITX (2-isopropylthioxanthone) were supplied by Great Lakes Fine Chemicals Ltd., Widnes, Cheshire while the Darocur 1173 (2-Hydroxy-2-methyl-1-phenyl-propan-1-one) was obtained from Ciba Specialty Chemicals, Manchester, UK. The diluent monomer resin, Actilane 430 (acrylated trimethylolpropane ethoxylate) was supplied by Akros Chemicals Company, Manchester, UK.

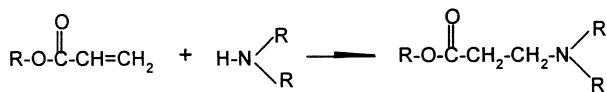
2.2. Synthesis of amine cosynergists

The amines investigated in this study are listed below and they were obtained from Aldrich Chemicals and Fluka Chemicals, except Tallowamine (coco-amine) which was supplied by Akros Chemicals, Eccles, Manchester, UK. For ease of identification during the following discussion the amine co-synergists will be given abbreviated names which are indicated in structures A to O.

A = $(C_2H_5)_2NH$	diethylamine
B = $(CH_3CH_2CH_2)_2NH$	dipropylamine
C = $(CH_3CH_2CH_2CH_2)_2NH$	dibutylamine
D = $CH_3-NH-CH_2-CH_2-OH$	2(methylamino)ethanol
E = $\text{NH}-\text{CH}_2-\text{CH}_2-\text{O}-\text{CH}_2-\text{CH}_2$	morpholine
F = $(CH_3CHOHCH_2)_2NH$	diisopropanolamine
G = TALLOWAMINE	primary amine
H = $[CH_3(CH_2)_5]_2NH$	dihexylamine
I = $(C_6H_{11})_2NH$	dicyclohexylamine
M = $[(CH_3)_2CH]_2NH$	diisopropylamine
N = 	1-methyl piperazine
O = 	4-methyl piperidine

Structures A to O for amine co-synergists.

The amine acrylates (co-synergists) were synthesised by the same general procedure. The synthesis was based on the Michael type addition of an amine to the 'activated'



Scheme 1. Michael type addition reaction.

acrylate double bond. The reaction can be represented as shown in Scheme 1.

The general procedure was as follows. The acrylated monomer to be reacted was charged into a flask and then the amine was added slowly. An immediate exothermic reaction was observed. The flask was placed into an oven at 65°C and periodically a sample of the reaction mixture was removed for titrimetric analysis. This analysis took the form of two non-aqueous titrations. The first titration gave a measure of the total amine content of the reaction mixture and the second titration differentiates between secondary and tertiary amine thereby giving an indication of the extent of the reaction and the amine value of the amine acrylate produced. Three different amine co-synergist concentrations were studied here depending upon the degree of sensitivity of the method of analysis for every amine used, starting with a B.V. = 25 and 100. More detailed examples of the methodologies used for the synthesis and the amine analysis are given in earlier papers [13–15].

2.3. Instrumentation techniques

2.3.1. Ultraviolet absorption measurements

Absorption spectra were obtained using a Perkin-Elmer Lambda 7 absorption spectrometer. UV spectroscopic studies were conducted by curing the resins onto optically flat quartz plates. Both normal (zero order) and second-order ($\delta^2 A / \delta \lambda^2$) derivative spectra were recorded using this equipment.

2.3.2. Infra-red measurements

Infra-red measurements were carried out using a BIO-RAD FTS-7 infra-red spectrometer. The secular reflectance spectra were recorded on cured surfaces. Infra-red was used to monitor the photooxidation index of cured coatings by the use of the following index:

$$\text{Degradation index} = \frac{\text{absorbance of monitored band}}{\text{absorbance of reference band}}$$

The reference band was used to compensate for film thickness variation and was found to be independent of cure conditions and photooxidation time. The monitored band was the hydroxyl band at $\sim 3450 \text{ cm}^{-1}$: this produce an hydroxyl index thus:

$$\text{Hydroxyl index} = \frac{\text{absorbance } 3450 \text{ cm}^{-1}}{\text{absorbance } 2940 \text{ cm}^{-1}}$$

The absorbance at 2940 cm^{-1} was used as the internal reference absorbance. The samples were coated on vacuum aluminised cardboard at $12 \mu\text{m}$ thickness.

2.3.3. Flash photolysis measurements

The use of a flash of light to induce photochemical reaction forms the basis of flash photolysis. Light absorption occurs very rapidly (10^{-4} s) but the decay processes cover a wider range of times from picoseconds for vibrational relaxation, to nanoseconds for radiative processes (from lower singlet state) and from microseconds to seconds for triplet decay processes, radicals and long-lived species. The concentration of transients is normally too low to be detected by their absorption spectra, but the use of a high intensity flash source can populate sufficiently the excited states to produce a high enough transient concentration to be measured by absorption spectroscopy. The monitoring sources switched on and a wavelength is selected at which the species of interest absorbs radiation. The photolysis lamp is then fired and the absorbance at this wavelength is observed on an oscilloscope. The wavelength can be changed as required to measure the absorbance of the intermediates at different wavelengths of interest.

2.4. Conventional microsecond flash photolysis

End of pulse transient absorption spectra were recorded using a conventional microsecond kinetic flash photolysis apparatus equipped with two 16 kV xenon filled flash lamps with 300 J energy output (operated at 10 kV) and a 150 W tungsten/halogen monitoring light source. Transient decay profiles were stored using a Gould model 1425 storage oscilloscope and the solutions were degassed using white spot nitrogen gas ($< 5 \text{ ppm O}_2$). Solutions were degassed using white spot nitrogen gas ($< 5 \text{ ppm O}_2$).

2.5. Irradiation unit

Microsca units were used during this study to photodegrade the radiation cured coatings. This unit utilised a 500W high pressure Hg/W lamp and operated at a temperature of 40°C and ambient humidity.

2.6. Hydroperoxide analysis

Hydroperoxide concentrations were estimated using the standard iodometric procedure, which is based on the reduction of hydroperoxides by sodium iodide in acetic acid medium. The concentration of I_3^- ions formed by this reaction can be measured spectrophotometrically.

A known mass (0.1–0.2 g) of coating was placed into a 50 cm³ round-bottom flask and refluxed for 30 min in propan-2-ol (9.5 cm³), glacial acetic acid (0.5 cm³) and sodium iodide (0.1 g). The iodine generated as I₃⁻ was measured spectrophotometrically at 420 nm against a control prepared in an identical manner. The concentration of hydroperoxide was read off a calibration curve prepared using cumene hydroperoxide as a standard. The samples were cured on aluminium plates at 60 μm thickness for study and analysis. This method was found to be satisfactory in previous work [8–10].

2.7. Real time infrared spectroscopy RTIR

The experimental set-up of the real time infrared photospectroscopy has been described in several recent papers [16,17]. The irradiation source used was a xenon lamp ILC 302UV (Laser Lines Ltd) connected to a dispersive infrared spectrophotometer. The lamp has a switched filter to irradiate with light above 400 nm using a fibre optic cable. Different samples were dissolved in a resin or a low viscosity acrylate, and were applied with calibrated wire bars on sodium chloride salt plates to give specific thickness and they were positioned uncovered in the sample holder. The chloride salt plates were placed in the reference beam in order to subtract the sodium chloride absorption from the sample.

Plots of conversion percentage and polymerisation rate versus irradiation time with light <400 nm were obtained. The maximum polymerisation rates (R_p maximum) were calculated from the slope of % conversion versus time plots at short irradiation times. For each sample replication has been done in order to have an estimation of the errors.

3. Results and discussion

3.1. Real time infrared spectroscopy

The photopolymerisation rates obtained via real time IR (RTIR) analysis are shown in Tables 1–3 for benzophenone, ITX and Darocur 1173 respectively at 2% w/w concentration. Here, the influence of the UV light, (wavelengths < 400 nm), as well as the effect of different photoinitiator addition are examined. The technique of RTIR spectroscopy is more applicable from a rate viewpoint for the comparison of the photopolymerisation ability of the initiators and the influence of amine type on cure.

In the case of benzophenone, the rate of photopolymerization decreased significantly in comparison with those of the other hydrogen atom abstracting Type II photoinitiator, ITX (isopropylthioxanthone). The Type I photofragmenting initiator Darocur 1173 was of intermediate activity in cure rates. The overall rates follow the

extent of absorption in the near UV region of the spectrum with ITX exhibiting the greatest absorption followed by Darocur 1173 and then benzophenone. As well as R_p values the conversion rates are also given after 40 s of irradiation time as well as the percentage unsaturation remaining. Thus, for benzophenone and ITX, the control Actilane 430 is the slowest curing system for R_p . However, for Darocur 1173 this is not the case. Conversion rates on the other hand are slower for the control resin, Actilane 430. All the amines accelerate cure due to the co-synergistic effect of the amine. The R_p values are related to the initial rates of cure and are more representative of the fast initial cure required industrially. The influence of amine structure is variable with initiator type across the three data tables. With benzophenone the highest R_p value is given with cocoamine whilst with ITX 4-methylpiperidine is the best followed by diisopropanolamine with Darocur 1173. The one interesting feature of the data however, is the low cure rate for all three initiator types in the presence of 1-methylpiperazine.

3.2. Conventional microsecond flash photolysis

The end-of-pulse transient absorption data (wavelength maxima and absorbances) of the acrylated amines in nitrogen-saturated propan-2-ol are shown in Table 4.

This analysis was undertaken only for the ITX since for benzophenone the formation of the radical anion species formed through electron transfer absorbs in the same region as the ketyl radical species. Photofragmenting initiators such as Darocur 1173 do not exhibit any triplet state and therefore, the influence of amine is not of significance here. End-of-pulse transient absorption spectra give rise to a strong maximum at 380 nm due to the ketyl radical of ITX. The Actilane 430 alone exhibits a strong quenching effect on the ketyl radical formation due to its interaction with the triplet state of the initiator. This can be collisional or via energy transfer processes. All the amines quench the ketyl radical formation with simple dialkyl amines being more effective than larger hindered structures. The ability of the amine group to form a triplet-exciplex with the ITX is important in the mechanism.

When the amine content was increased as seen in Table 5, the hydrogen atom abstraction decreased drastically because the amine is in excess over the initiator.

All the amines quenched the triplet processes through exciplex formation, to give the semiquinone radical and very weak radical anion species. Primary amines were generally more effective quenchers than the cycloaliphatic ones which prove to give high values of semiquinone radicals. The radical anion formation, which absorbs at wavelengths higher than 400 nm was evident although weak when compared to that of the control Actilane 430 on its own.

Table 1
RTIR results in the presence of 2% w/w benzophenone as the photoinitiator

Sample (B.V. = 25)/2% benzophenone	R_p max (mol l ⁻¹ s ⁻¹)	% Conversion at 40 s	% Unsaturation at 40 s
Act 430	0.31 +/- 0.2	19.2	80.8 +/- 0.5
Diethylamine (A)	5.07	49.1	50.9
Dipropylamine (B)	4.3	44	56
Diisopropylamine (M)	5.81	41.3	58.7
Diisopropanolamine (F)	4.45	40.8	59.2
Dibutylamine (C)	4.78	52.3	47.7
2(Methylamino)ethanol (D)	4.21	39.7	60.3
Morpholine (E)	5.83	41.3	58.7
Coco-amine (G)	7.18	68.1	31.9
Dihexylamine (H)	4.06	37.2	62.8
Dicyclohexylamine (I)	6.96	42.5	57.5
1-Methyl piperazine (N)	1.96	45	55
4-Methyl piperidine (O)	4.52	42	58

Table 2
RTIR results in the presence of 2% w/w ITX

Sample (B.V. = 25)/2% ITX	R_p max (mol l ⁻¹ s ⁻¹)	% Conversion at 40 s	% Unsaturation at 40 s
Act 430	6.25 +/- 0.2	42.6	57.4 +/- 0.5
Diethylamine (A)	12.83	80.8	19.2
Dipropylamine (B)	17.2	80.8	19.2
Diisopropylamine (M)	13.27	74.6	25.4
Diisopropanolamine (F)	16.44	82.6	17.4
Dibutylamine (C)	18.22	79.2	20.8
2(Methylamino)ethanol (D)	16.8	87.3	12.7
Morpholine (E)	13.54	81.1	18.8
Coco-amine (G)	16	83.8	16.2
Dihexylamine (H)	15.53	80.7	19.3
Dicyclohexylamine (I)	4.23	52.9	47.1
1-Methyl piperazine (N)	9.35	74.6	25.4
4-Methyl piperidine (O)	18.4	86.8	13.2

Table 3
RTIR results in the presence of 2% w/w Daracur 1173

Sample (B.V. = 25)/2% Daracur 1173	R_p max (mol l ⁻¹ s ⁻¹)	% Conversion at 40 s	% Unsaturation at 40 s
Act 430	10.5 +/- 0.2	13.8	86.2 +/- 0.5
Diethylamine (A)	10.1	72	28
Dipropylamine (B)	12.35	66.2	33.8
Diisopropylamine (M)	9.92	69.7	30.3
Diisopropanolamine (F)	14.58	74.1	25.9
Dibutylamine (C)	13.72	72.7	27.3
2(Methylamino)ethanol (D)	11.12	76.2	23.8
Morpholine (E)	12.06	71.5	28.5
Coco-amine (G)	11.53	75	25
Dihexylamine (H)	10.55	58.9	41.1
Dicyclohexylamine (I)	7.77	34.6	65.4
1-Methyl piperazine (N)	7.5	50.5	49.5
4-Methyl piperidine (O)	9.87	60.6	39.4

3.3. FTIR spectroscopy

The hydroxyl index was used as a measure of the relative rates of photodegradation and/or photooxida-

tion of UV and EB cured coatings and was not undertaken in previous studies. Here the influence of the amine structure was evident. As mentioned in the previous section, the relative intensity of the band situated

at $\sim 2940\text{ cm}^{-1}$ remained constant during irradiation and was considered as an internal standard to compensate for slight variations in sample thickness and to allow different samples to be compared directly.

All samples, UV or EB cured, were photodegraded in a microscal unit and the photodegradation was monitored quantitatively by reflectance infra-red spectroscopy (RFTIR).

The effect of microscal irradiation on the hydroxyl index is illustrated in Figs. 1–4 for the UV cured coatings while those in Figs. 5–8 show changes for those that had been EB cured. The most striking feature of this data is the similarity of the photodegradation profile on the nature of the curing process. Thus, samples that had been UV and EB cured exhibited similar profiles with the same amine structure (all with a B.V of 100). This suggests that apart from the initial effects of residual photoinitiator in the UV cured coatings the amine structure has a marked controlling influence on the rate of oxidation.

Table 4

Transient absorption maxima and absorbances on conventional microsecond flash photolysis in nitrogen saturated propan-2-ol for a base value of 25 (in presence of ITX as initiator)

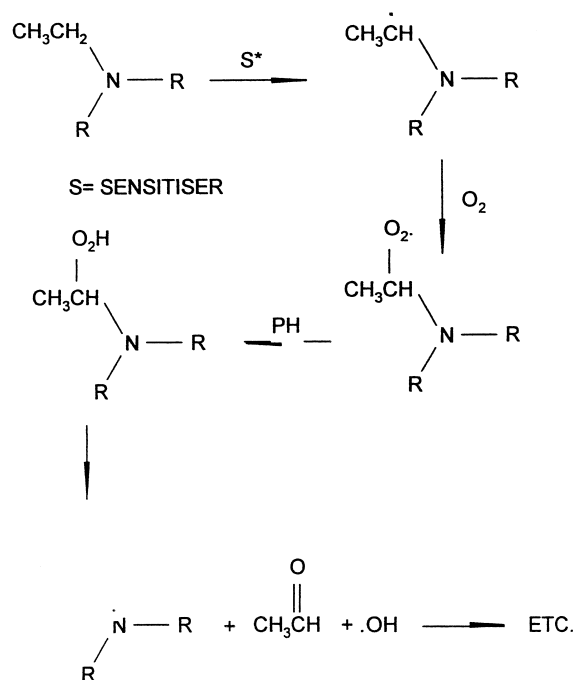
Sample	Absorption maximum λ_{max} (nm)	Absorbance
ITX	370	0.698
Act 430	380	0.255
Diethylamine (A)	380	0.128
Dipropylamine (B)	380	0.154
Diisopropylamine (M)	380	0.269
Diisopropanolamine (F)	380	0.121
Dibutylamine (C)	380	0.131
2(Methylamino)ethanol (D)	380	0.128
Morpholine (E)	370	0.134
Coco-amine (G)	380	0.145
Dihexylamine (H)	380	0.132
Dicyclohexylamine (I)	380	0.255
1-Methyl piperazine (N)	380	0.238
4-Methyl piperidine (O)	380	0.218

Table 5

Transient absorption maxima and absorbances on conventional microsecond flash photolysis in nitrogen-saturated propan-2-ol for a 30% amine content (in presence of ITX as initiator)

Act 430	Absorption maximum λ_{max} (nm)	Absorbance
/	380	0.255
Diethylamine (A)	360	0.052
Dipropylamine (B)	370	0.061
Diisopropanolamine (F)	370	0.066
Dibutylamine (C)	360	0.059
2(Methylamino)ethanol (D)	370	0.067
Morpholine (E)	360	0.117
Dicyclohexylamine (I)	360	0.061
1-Methyl piperazine (N)	380	0.019
4-Methyl piperidine (O)	360	0.059

Most of the UV cured coatings exhibited an initial rapid increase in hydroxyl growth followed by a decline and then a very gradual increase or plateau effect. The control Actilane 430 with no amine exhibited a gradual increase in hydroxyl index and was overall the greatest effect compared with the amine-terminated acrylates. This suggests that all the amine acrylates imparted some degree of oxidative photostability to the cured films. This is associated with the oxygen scavenging ability of the tertiary amine structure where the initially generated alkylamino radicals react rapidly with oxygen to form unstable hydroperoxides. These, break down rapidly generating aldehydes. In the case of diethylamine acetaldehyde would be formed. Depending upon the efficiency of the amine structure the scavenging effect may significantly inhibit oxidation of the backbone structure of the resin and hence localise oxidation at the chain ends. This may be exemplified by an autoretarding effect, often seen with for example, hindered piperidine light stabilisers in commercial plastics [18]. A rapid initial growth in hydroxyl index is seen for the resin containing 2-methylaminoethanol (Fig. 1) and 1-methylpiperazine (Fig. 4). The common feature in these two systems is the presence of an *N*-methyl group, which could oxidise rapidly to give formaldehyde (as for reaction shown, Scheme 2). The morpholine derivative also exhibited a marked initial rise in hydroxyl growth and this may be due to the presence of the ring ether link, which can oxidise rapidly. All three simple dialkylamines (diethyl, dipropyl and di-*n*-butyl) (Fig. 2) exhibit a gradual rise in hydroxyl index with irradiation time.



Scheme 2. Oxidation of tertiary amine structure.

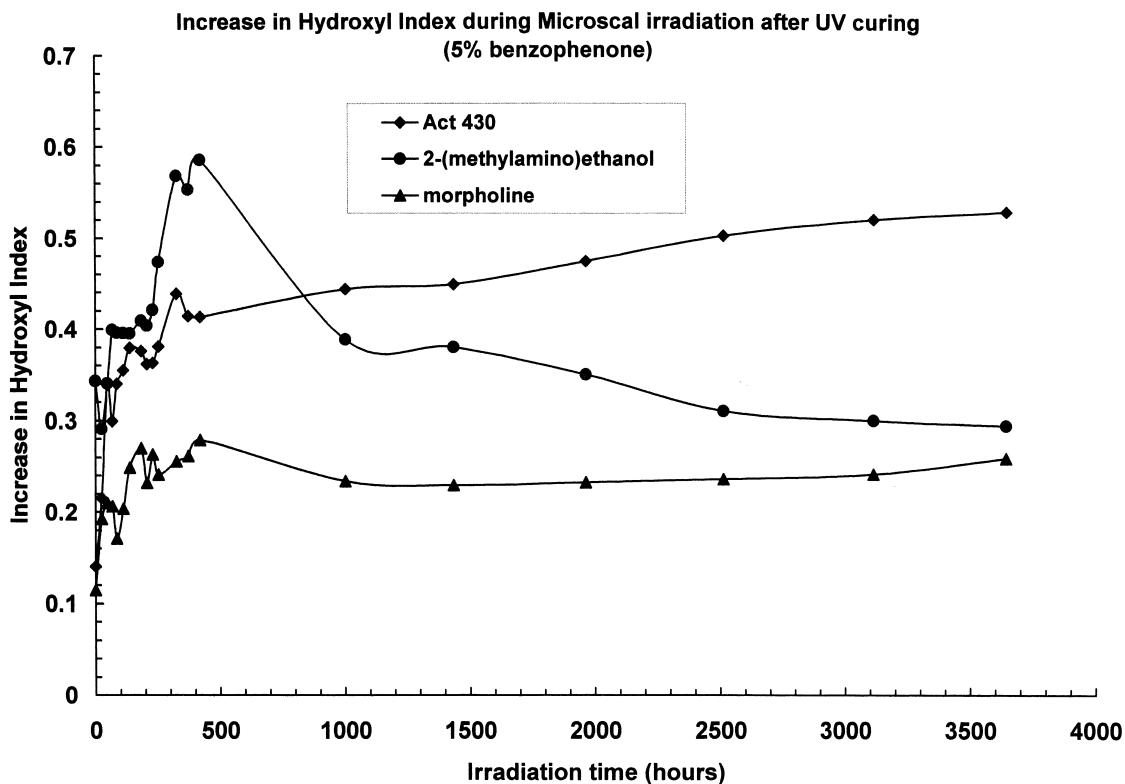


Fig. 1. Hydroxyl index versus irradiation time (h) for (◆) Actilane 430, (●) 2-methylaminoethanol and (▲) morpholine terminated Actilane 430 (100 B.V.) after UV curing (5% w/w benzophenone).

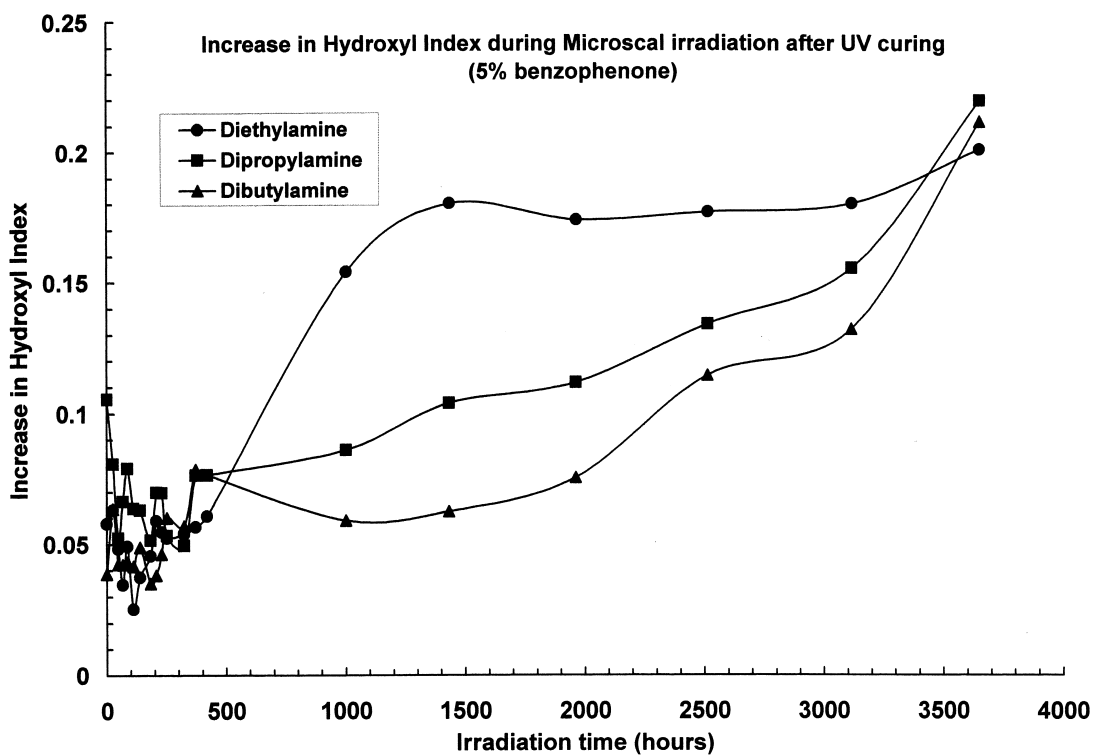


Fig. 2. Hydroxyl index versus irradiation time (h) for (◆) diethylamine, (●) dipropylamine and (▲) dibutylamine terminated Actilane 430 (100 B.V.) after UV curing (5% w/w benzophenone).

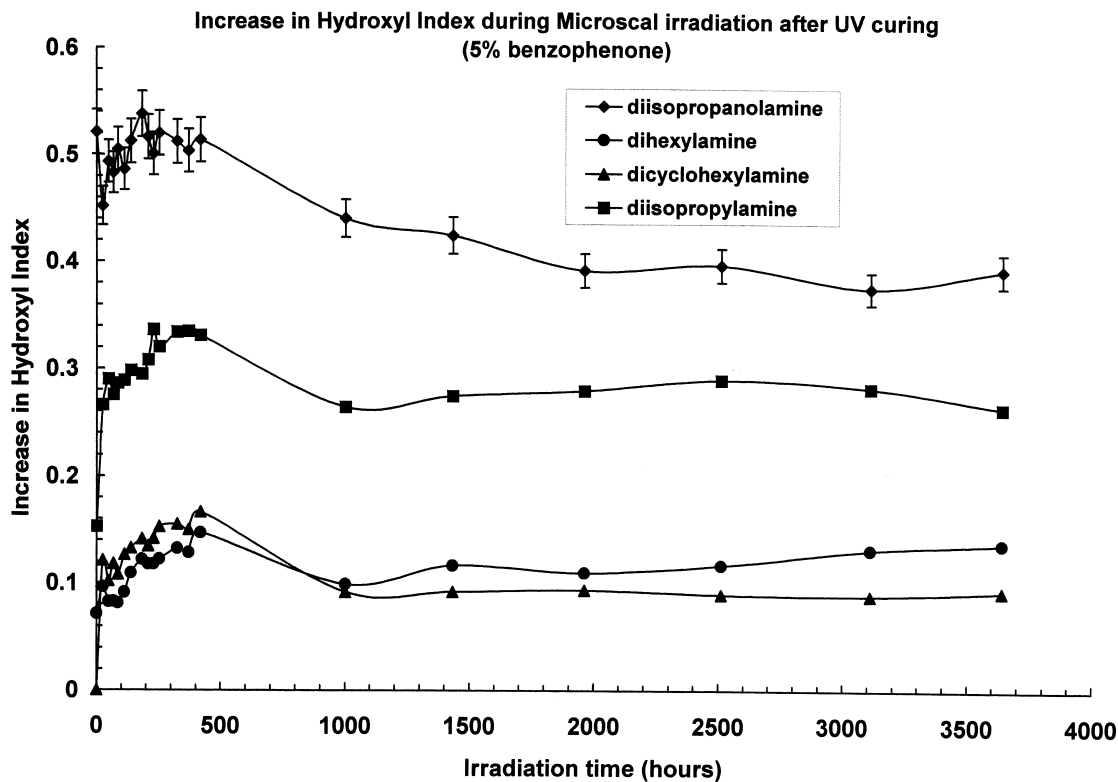


Fig. 3. Hydroxyl index versus irradiation time (h) for (♦) diisopropanolamine, (●) dihexylamine, (▲) dicyclohexylamine and (■) diisopropylamine terminated Actilane 430 (100 B.V.) after UV curing (5% w/w benzophenone).

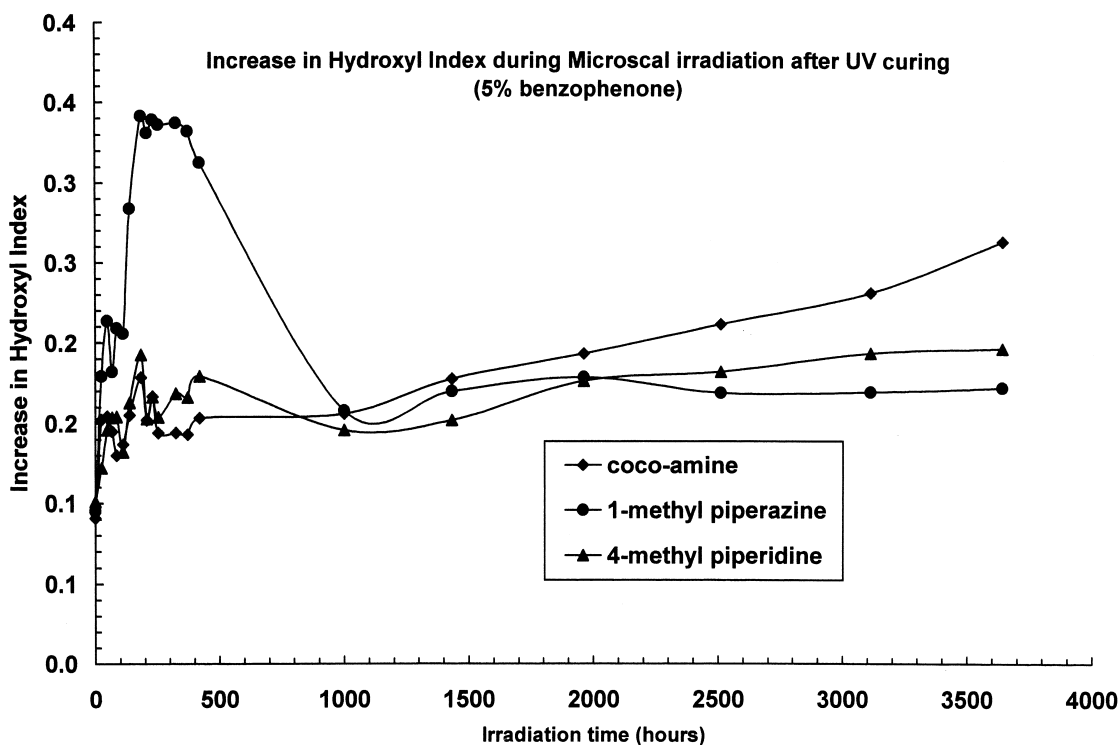


Fig. 4. Hydroxyl index versus irradiation time (h) for (♦) cocoamine, (●) 1-methylpiperazine and (▲) 4-methylpiperidine terminated Actilane 430 (100 B.V.) after UV curing (5% w/w benzophenone).

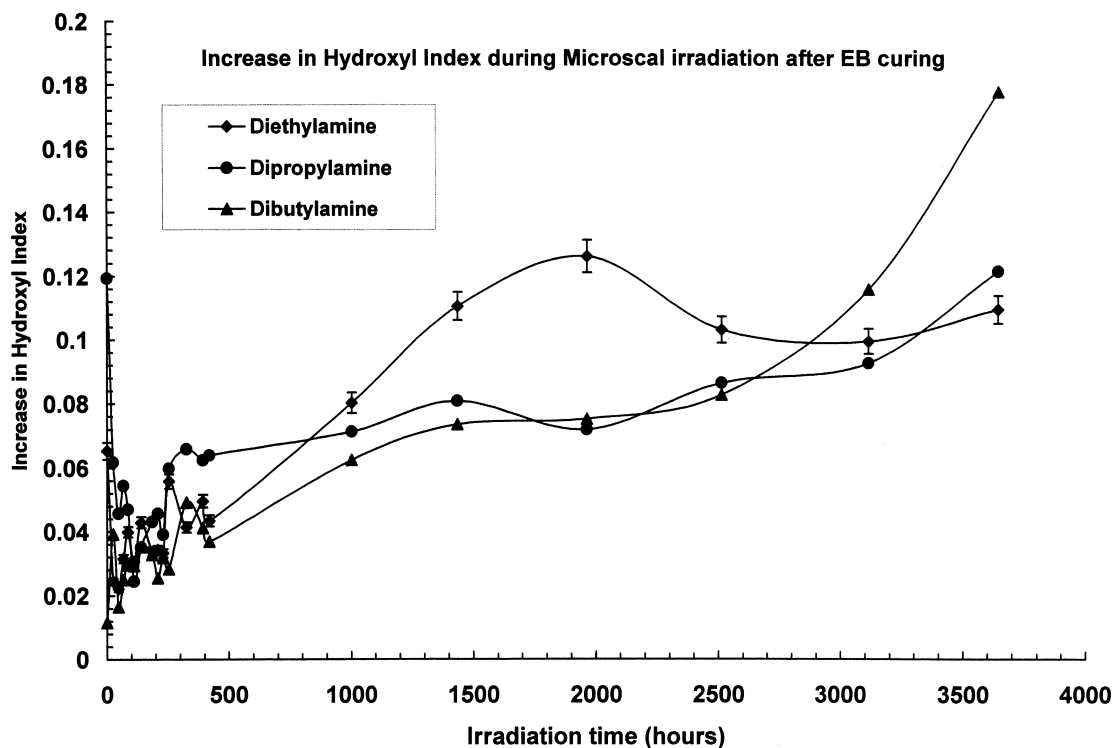


Fig. 5. Hydroxyl index versus irradiation time (h) for (♦) diethylamine, (●) dipropylamine and (▲) dibutylamine terminated Actilane 430 (100 B.V.) after EB curing.

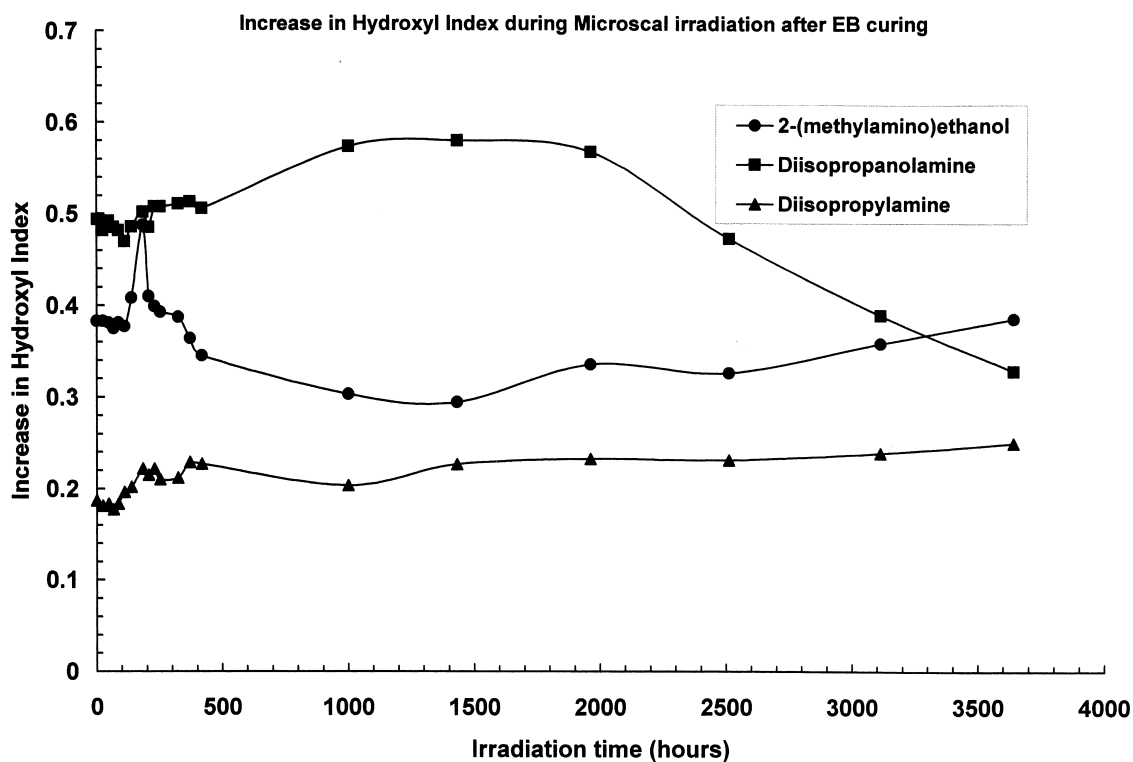


Fig. 6. Hydroxyl index versus irradiation time (h) for (●) 2-(methylamino)ethanol, (■) diisopropanolamine and (▲) diisopropylamine terminated Actilane 430 (100 B.V.) after EB curing.

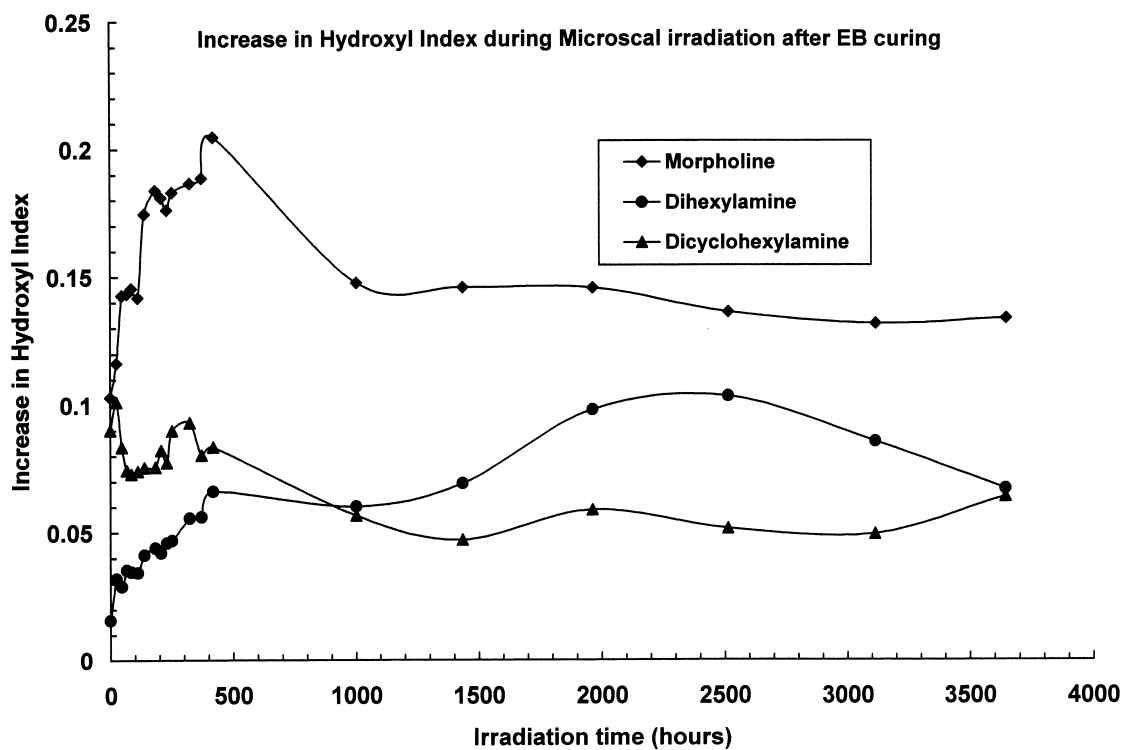


Fig. 7. Hydroxyl index versus irradiation time (h) for (♦) morpholine, (●) dihexylamine and (▲) dicyclohexylamine terminated Actilane 430 (100 B.V.) after EB curing.

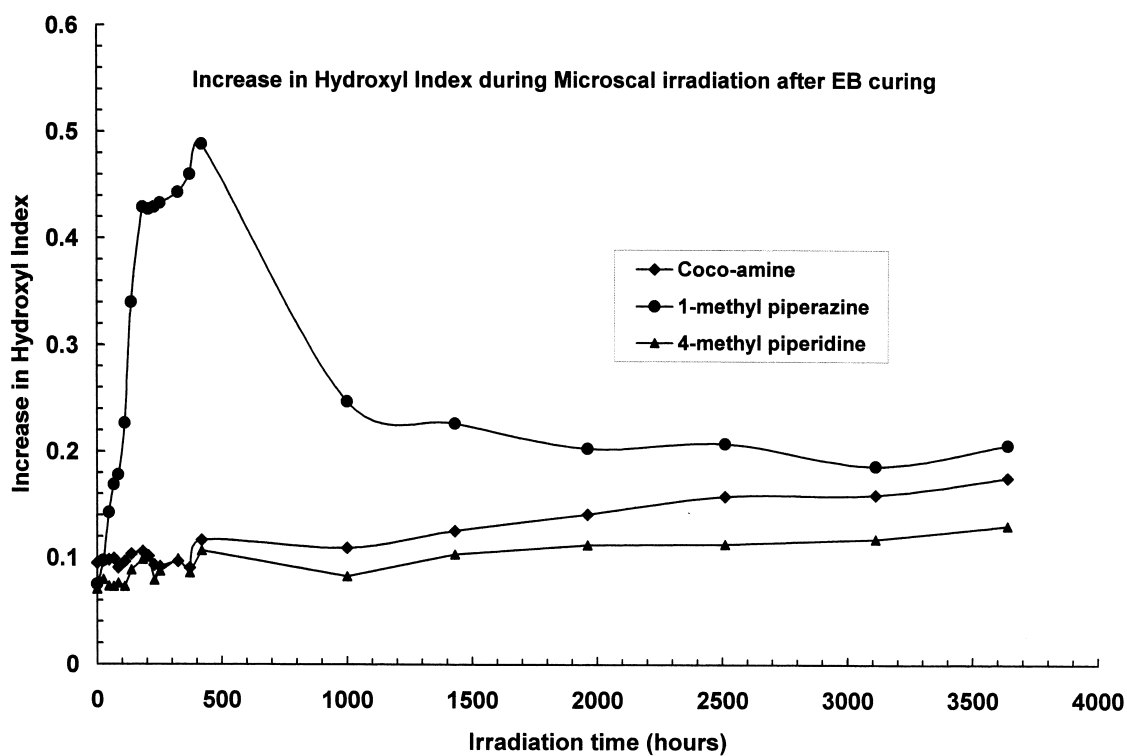


Fig. 8. Hydroxyl index versus irradiation time (h) for (♦) cocoamine, (●) 1-methylpiperazine and (▲) 4-methylpiperidine terminated Actilane 430 (100 B.V.) after EB curing.

The dihexyl and cocoamine derivatives appear to be much more stable.

For the EB cured systems again the terminal amine structure exhibited a strong stabilising effect on the coating. As for the UV cured coatings the three simple dialkylamine containing resins exhibited a gradual increase in hydroxyl index with the diethyl derivative exhibiting the greatest increase.

Hydroxyl index changes for the EB cured samples are illustrated in Figs. 5–8.

For some of the EB cured samples there is an initial rapid reduction in OH and this is due to an initial loss of moisture induced by the heating of the lamp. All the dialkylamines exhibit a gradual increase in OH formation while the long chain cocoamine system exhibits a much slower rate in comparison. The other amines, 4-methylpiperidine, dicyclohexylamine and diisopropylamine exhibit little or no overall change. and For the 1-methyl piperazine and morpholine acrylates photodegradation processes involves an initial rapid production of hydroxyl species in the coating followed by a decrease and afterwards a gradual decrease. The 2-methylaminoethanol terminated coating also exhibits a very rapid initial rise in OH followed by a decrease and then slow incline. These changes were also evident in the UV cured coatings confirming the dominant effect of the amine structure on the relative rates of oxidation.

3.4. Hydroperoxide measurements

In UV and EB cured coatings, hydroperoxides may be incorporated into the cured coating during the curing process, as oxygen in the coating scavenges initiating radicals. They may play an important role in the photodegradation of these coatings. They will also play an intermediate role during the irradiation process and therefore, make an interesting comparison with the hydroxyl index. The analysis of hydroperoxides in radiation-cured coatings is extremely difficult from a practical point-of-view. Irradiated coatings have to be removed by scraping thin film fragments from pre-coated aluminium plates. Following refluxing in acidic-isopropanol solution the fragments then have to be removed by rapid filtration through fine PTFE syringe filters directly into the UV cell for measurement. Each measurement was carried out in triplicate and consequently the method was applied for study to specific resin systems. These are compared for both UV and EB cured coatings in Figs. 9–13.

As can be seen from the Figures there are less initial hydroperoxides in EB cured films than those, which had been UV cured. In UV cured films the initial hydroperoxides produced during the curing process decompose rapidly on irradiation and are therefore photolabile (Figs. 9–11). The only exception was that containing the

1-methylpiperazine which exhibited an initial high value of hydroperoxide which on irradiation increases slowly up to 26 h and, thereafter, decreases rapidly followed by a rapid increase and further decrease. All the UV cured resins, in fact, exhibit an initial early rise in hydroperoxide concentration followed by a gradual decline. This is to be expected based on the reaction scheme 2 illustrating their high instability [12–15]. A very low level is present after the initial decay, but *N* (1-methyl piperazine) gives rise to the highest concentration of hydroperoxides for both curing methods. In the EB cured films, the hydroperoxide level is very small after curing, but during irradiation they increase and later decrease rapidly to a small level. The EB systems show a rapid initial hydroperoxidation and, thereafter, a decrease — an effect, which is amine structure dependant (Figs. 11 and 13). The dipropylamine containing EB cured system exhibits the most rapid rise but the peroxides are, as expected, unstable and variations are periodically observed. The 2-methylaminoethanol, diethylamine and 4-methylpiperidine systems fluctuated during irradiation but at a very low concentration level when compared with the corresponding UV cured resins. Such differentials in hydroperoxide were reported in our earlier work on diethylamine-terminated resins [12–15]. Initial fluctuations in the OH measurements are therefore, expected on the basis of the variable instabilities of the hydroperoxides.

3.5. Second-order derivative UV spectroscopy

Three different amine concentrations were examined in this study in order to examine the influence of amine concentration on the rate of formation of the derivative UV absorption band at 275 nm. This band corresponds to a higher energy transition of the species believed to be responsible for yellow product in the amine-acrylated coatings [12–15]. UV cured coatings with a BV of 25 could not be examined by UV analysis due the insensitivity of the method associated with the strong interference by the residual benzophenone initiator. These were examined at a BV=100 and the processes observed here are significant over the early stages of the photooxidation.

From our earlier studies [12–15] EB cured amine acrylated coatings exhibited a gradual increase in the UV absorption band at 275 nm and thereafter decreased to a steady-state. This effect was generally evident in this study for all the amine acrylates examined here with a BV = 25. The data are plotted in Figs. 14–17. All the dialkylamines exhibited the highest absorption changes and this effect is consistent with our earlier work. Co-reaction with cocoamine was no exception and showed a continual rise in UV absorption. Both the alkanolamines and heterocyclic amines exhibited lower overall increases in UV absorption except morpholine.

Amine acrylated resins with a BV=100 were also studied to determine the effect of amine concentration on UV absorption growth. The results are compared in

Figs. 18 and 19 for the different amine systems. These systems exhibit significantly higher UV absorption values and clearly relate discolouration to the terminal

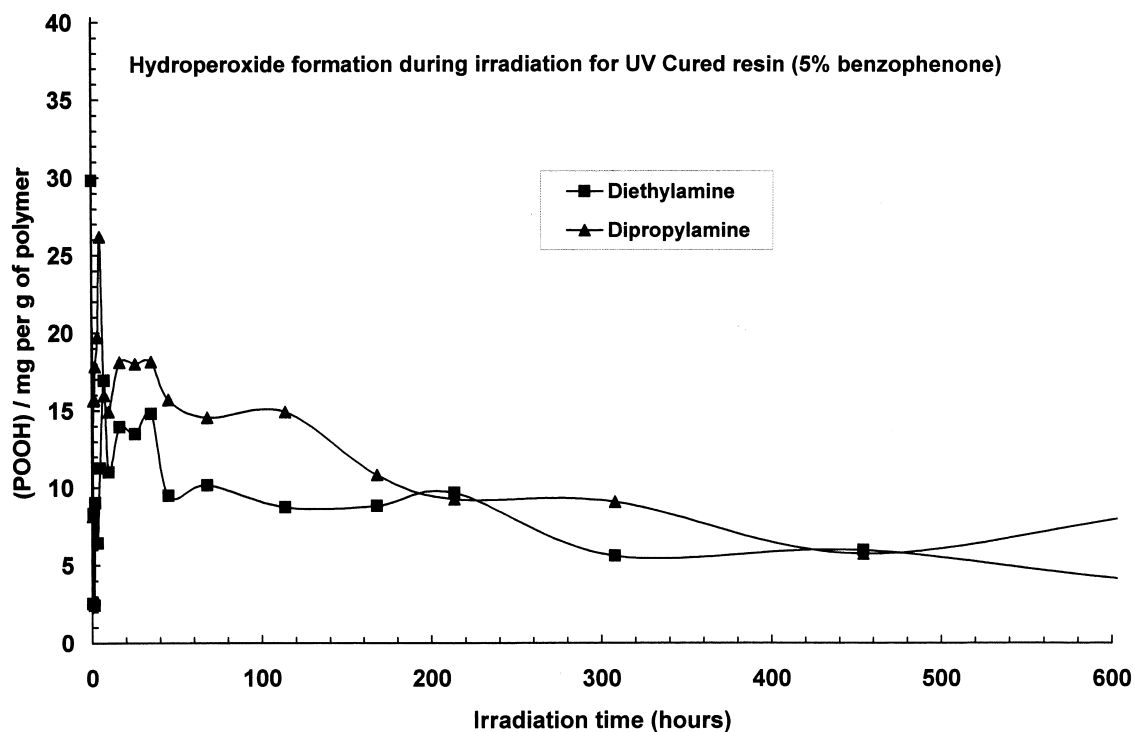


Fig. 9. Hydroperoxide concentration versus irradiation time (h) for (■) diethylamine and (▲) dipropylamine terminated Actilane 430 (100 BV) after UV curing (5% w/w benzophenone).

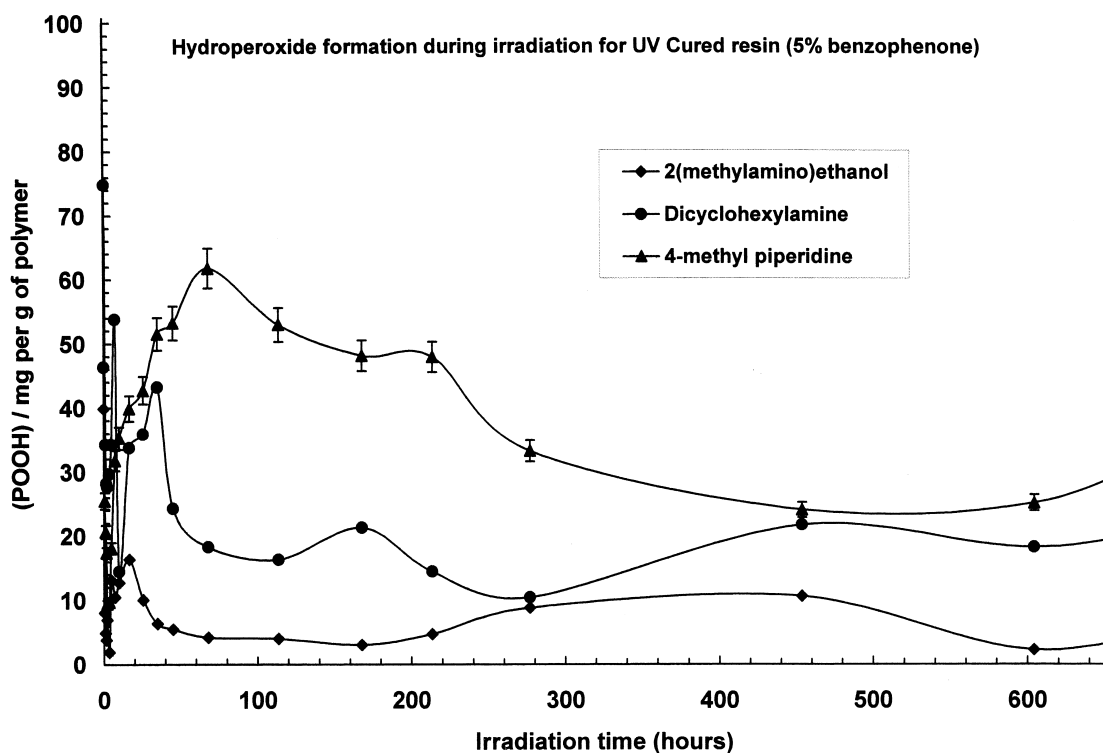


Fig. 10. Hydroperoxide concentration versus irradiation time (h) for (◆) 2-methylaminoethanol, (●) dicyclohexylamine and (▲) 4-methylpiperidine terminated Actilane 430 (100 B.V.) after UV curing (5% w/w benzophenone).

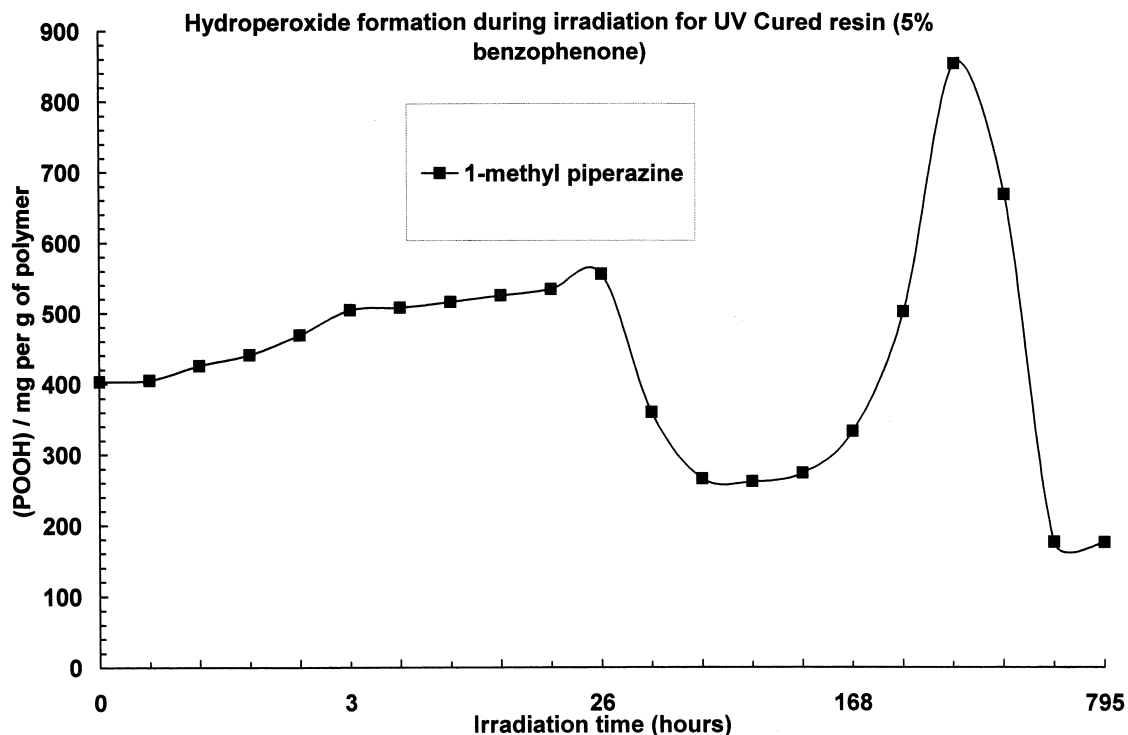


Fig. 11. Hydroperoxide concentration versus irradiation time (h) for (■) 1-methylpiperazine terminated Actilane 430 (100 B.V.) after UV curing (5% w/w benzophenone).

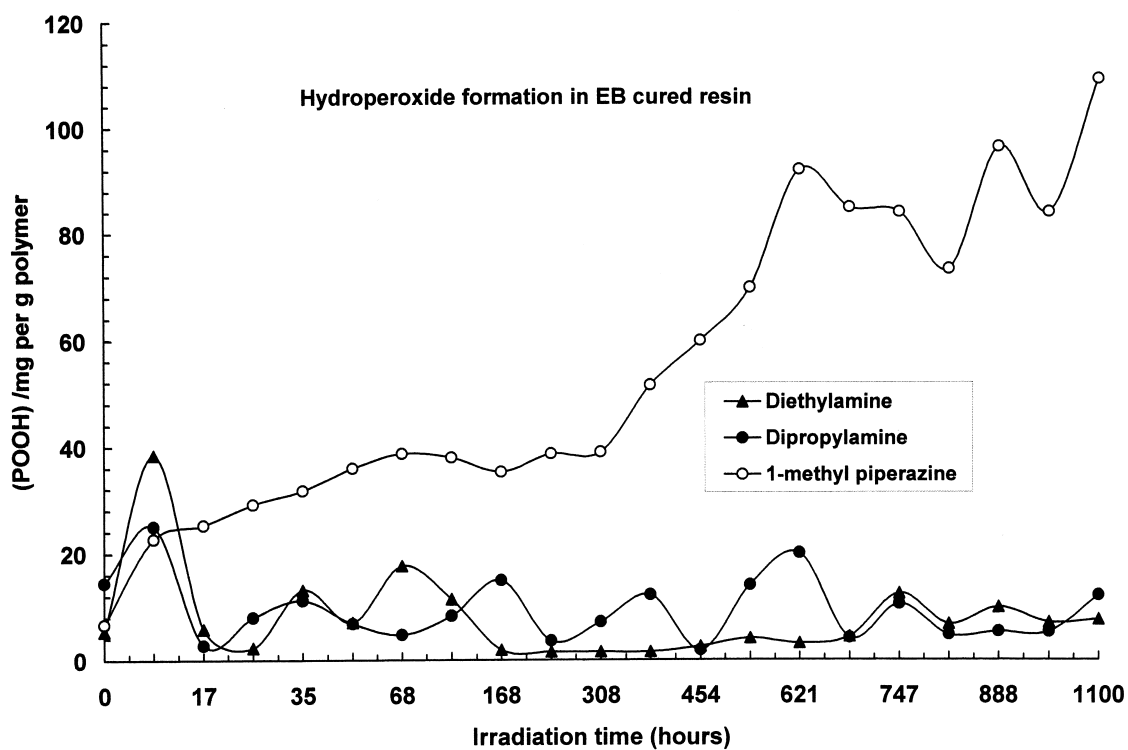


Fig. 12. Hydroperoxide concentration versus irradiation time (h) for (▲) diethylamine, (●) dipropylamine and (○) 1-methylpiperazine terminated Actilane 430 (100 B.V.) after EB curing.

Hydroperoxides formation in EB curing

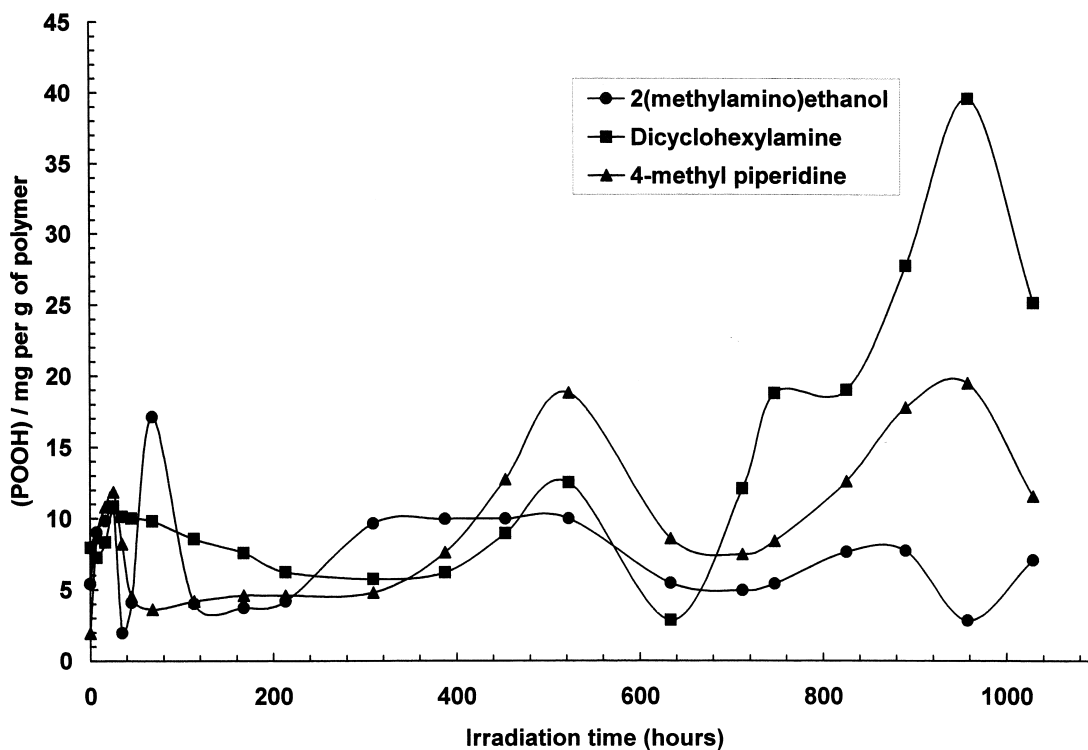


Fig. 13. Hydroperoxide concentration versus irradiation time (h) for (●) 2-methylaminoethanol, (■) dicyclohexylamine and (▲) 4-methylpiperidine terminated Actilane 430 (100 B.V.) after EB curing.

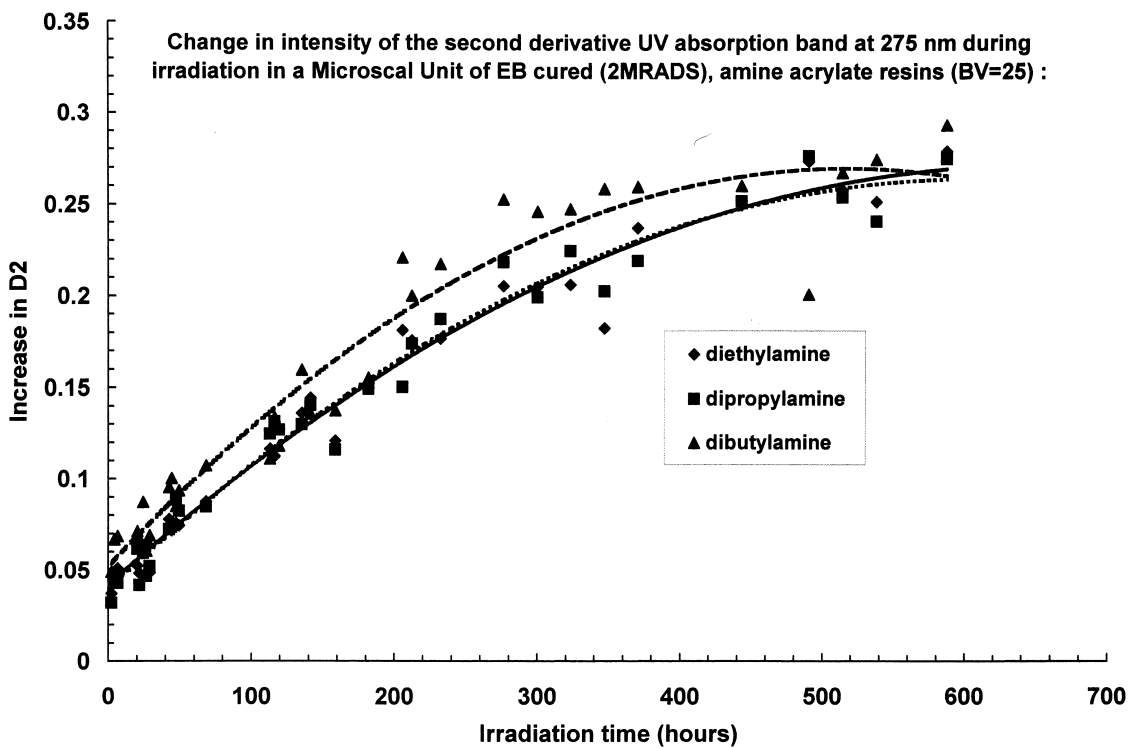


Fig. 14. Second order derivative UV absorption at 275 nm versus irradiation time for (◆) diethylamine, (■) dipropylamine and (▲) dibutylamine terminated Actilane 430 resin EB cured (B.V. = 25).

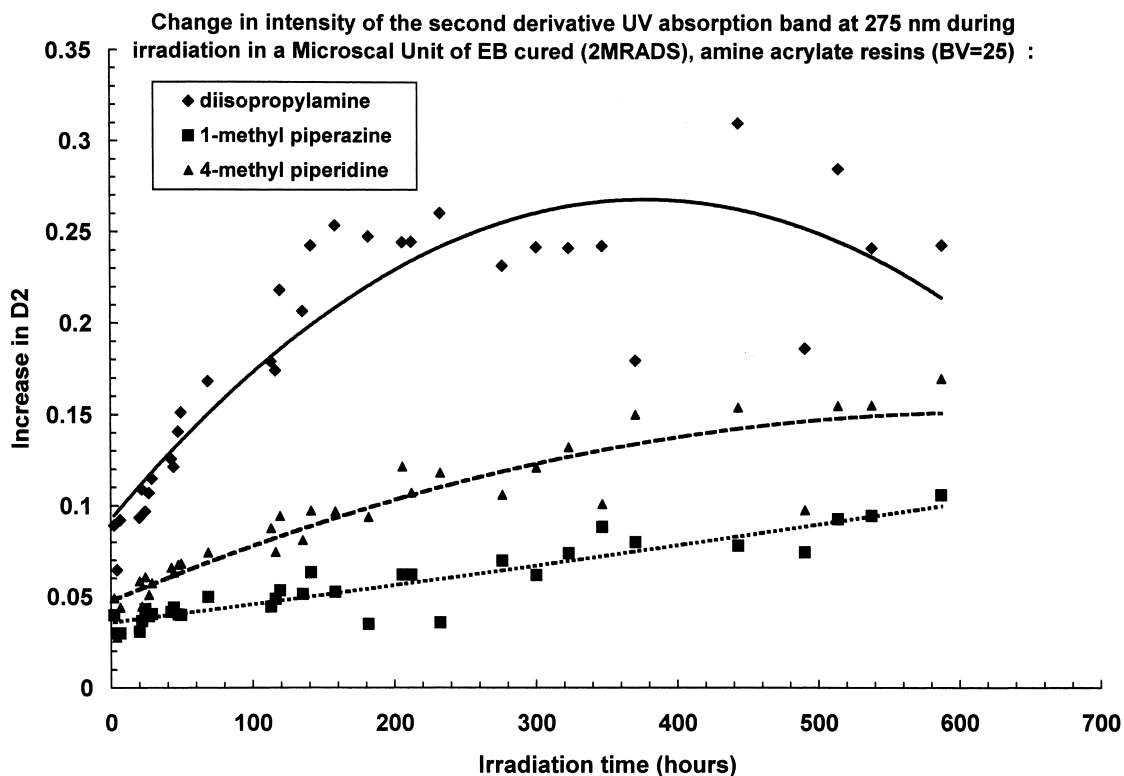


Fig. 15. Second order derivative UV absorption at 275 nm versus irradiation time for (◆) diisopropylamine, (■) 1-methylpiperazine and (▲) 4-methylpiperidine terminated Actilane 430 resin EB cured (B.V. = 25).

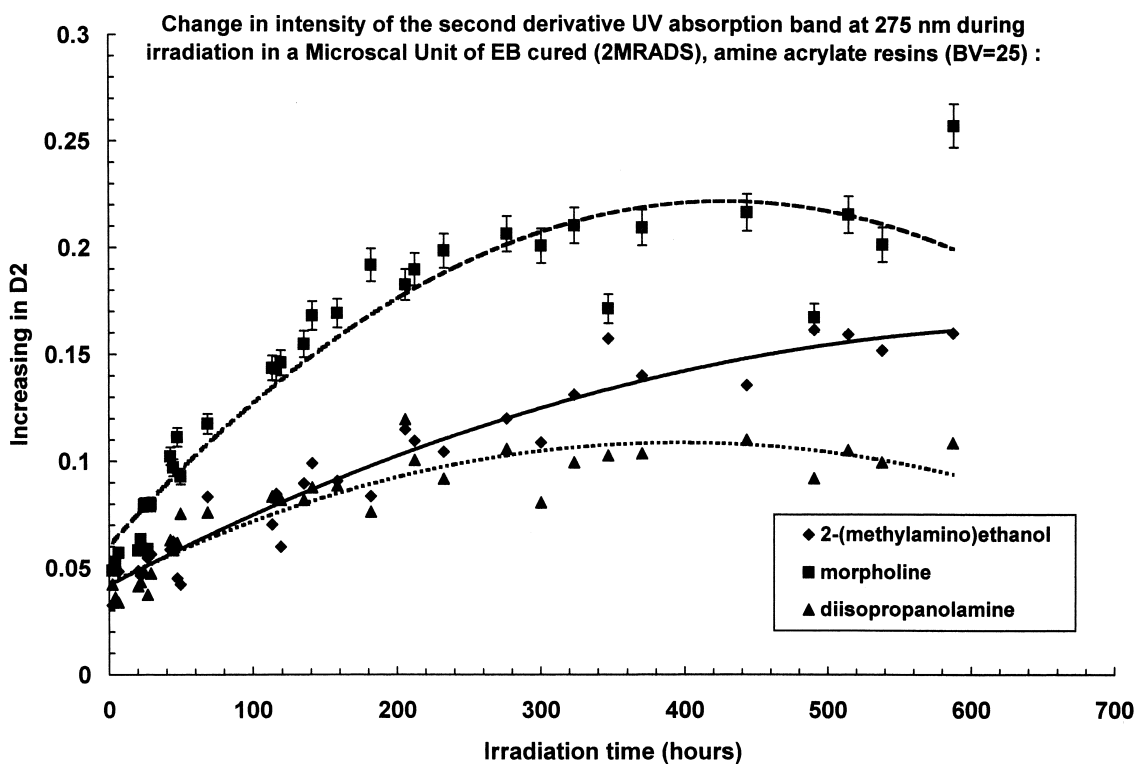


Fig. 16. Second order derivative UV absorption at 275 nm versus irradiation time for (◆) 2-methylaminoethanol, (■) morpholine and (▲) diisopropanolamine terminated Actilane 430 resin EB cured (B.V. = 25).

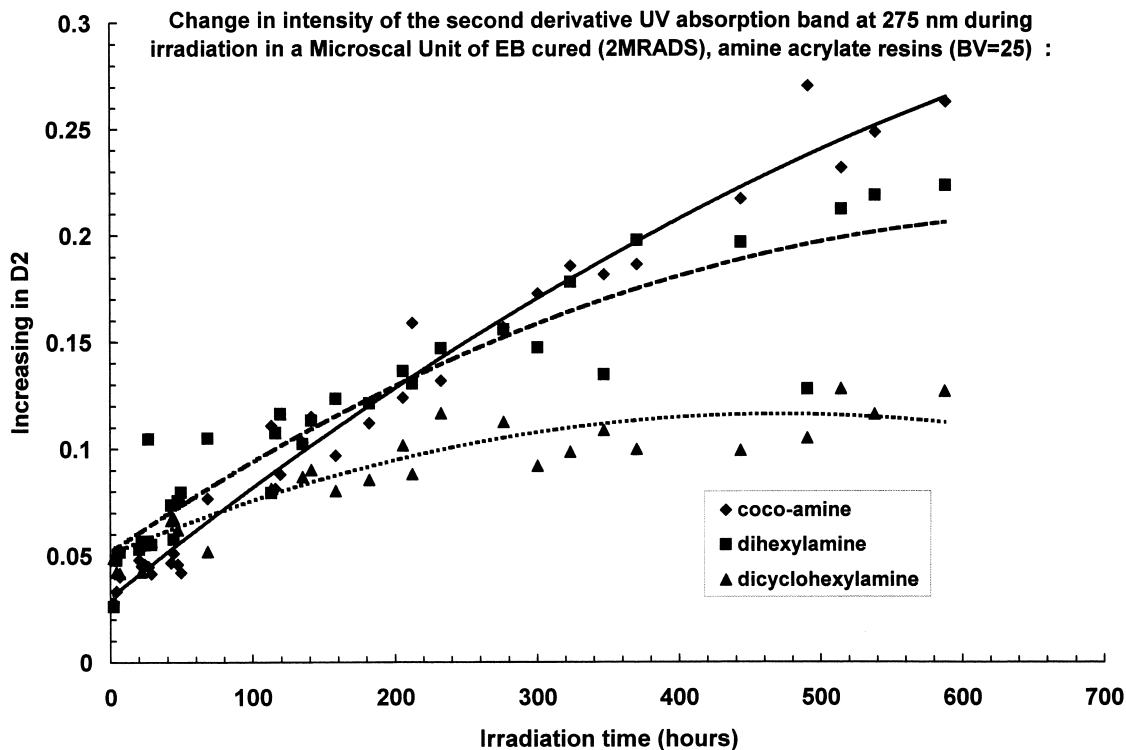


Fig. 17. Second order derivative UV absorption at 275 nm versus irradiation time for (◆) cocoamine, (■) dihexylamine and (▲) dicyclohexylamine terminated Actilane 430 resin EB cured (B.V. = 25).

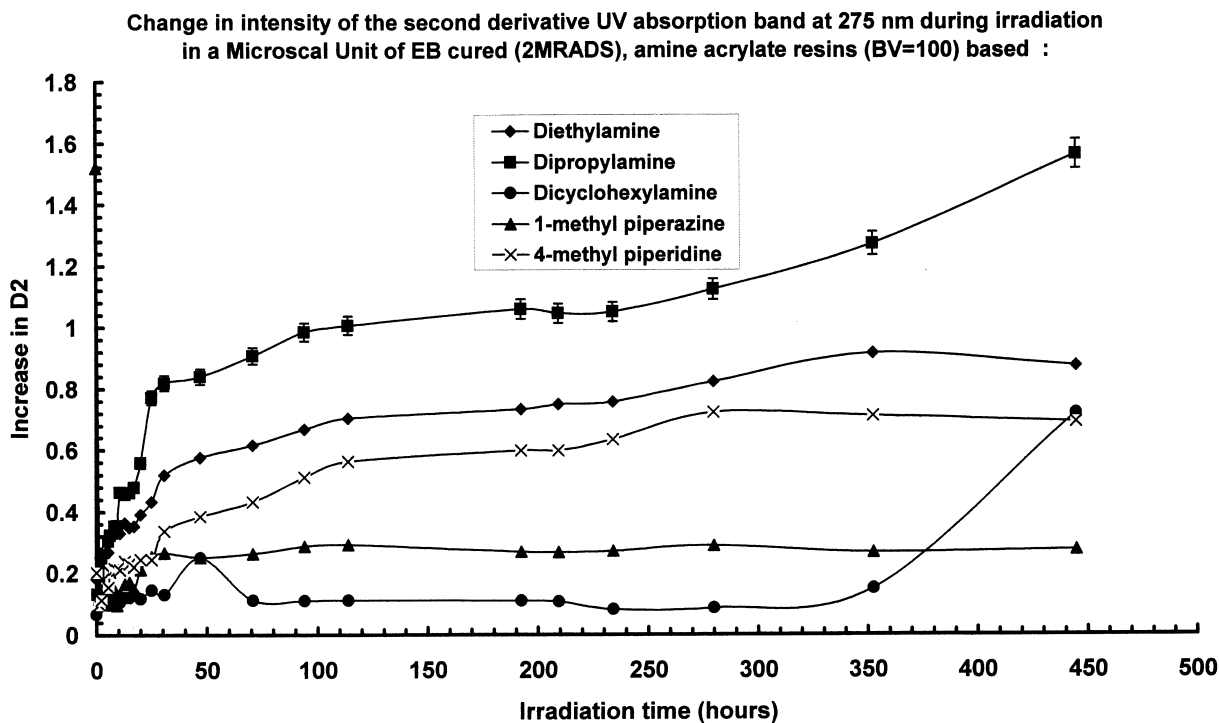


Fig. 18. Second order derivative UV absorption at 275 nm versus irradiation time for (◆) diethylamine, (■) dipropylamine, (●) dicyclohexylamine, (▲) 1-methylpiperazine and (×) 4-methylpiperidine terminated Actilane 430 resin EB cured (BV = 100).

amine group concentration. All the amine systems here exhibit very gradual increases in UV absorption the extent of which is dependent upon the amine structure.

The only exception is dihexylamine, which shows an initial rapid rise in UV absorption over the first 5 h and, thereafter, a very gradual decline. Again, the dialkyl-

amines exhibit the highest rate increases as does morpholine. The alkanolamines exhibit the lowest rate increase as does dicyclohexylamine. Alkanolamines are

generally known to be less prone to yellowing than their dialkyl analogues. In the case of dicyclohexylamine steric effects to oxidation are considered possible.

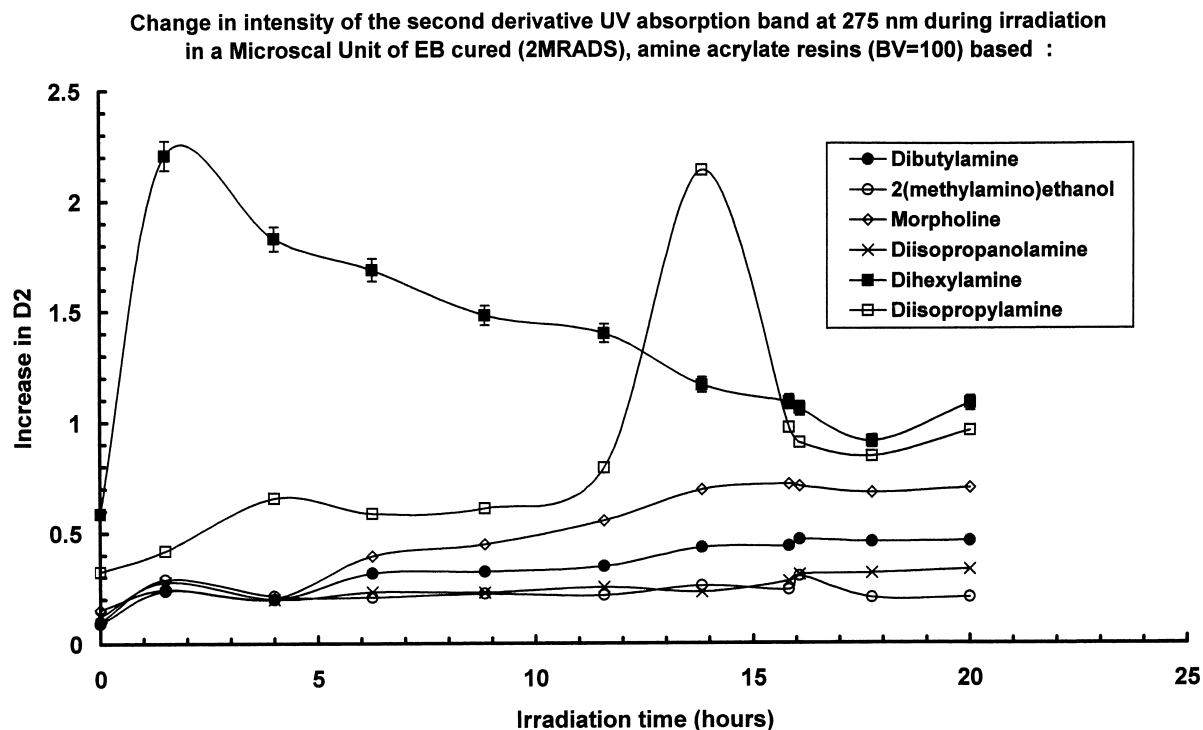


Fig. 19. Second order derivative UV absorption at 275 nm versus irradiation time for (●) dibutylamine, (○) 2-methylaminoethanol, (◇) morpholine, (×) diisopropanolamine, (■) dihexylamine, (□) diisopropylamine terminated Actilane 430 resin EB cured (B.V. = 100).

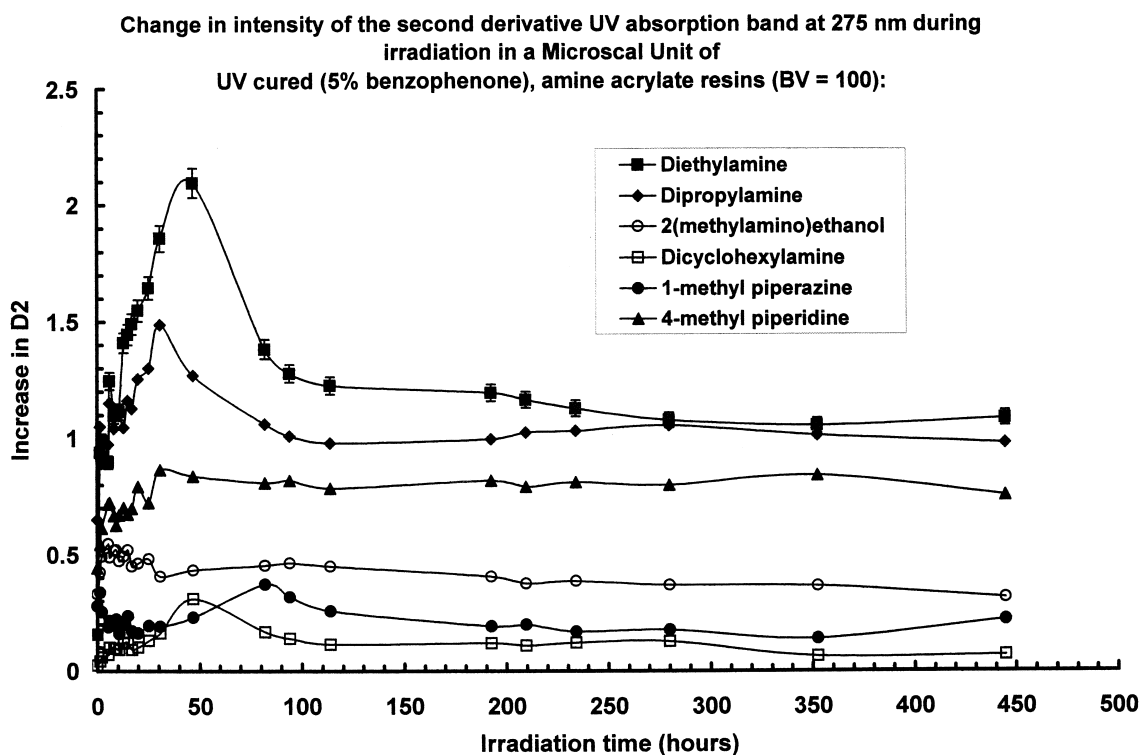


Fig. 20. Second order derivative UV absorption at 275 nm versus irradiation time for (■) diethylamine, (◆) dipropylamine, (○) 2-methylaminoethanol, (□) dicyclohexylamine, (●) 1-methylpiperazine and (▲) 4-methylpiperidine terminated Actilane 430 resin EB cured (B.V. = 100).

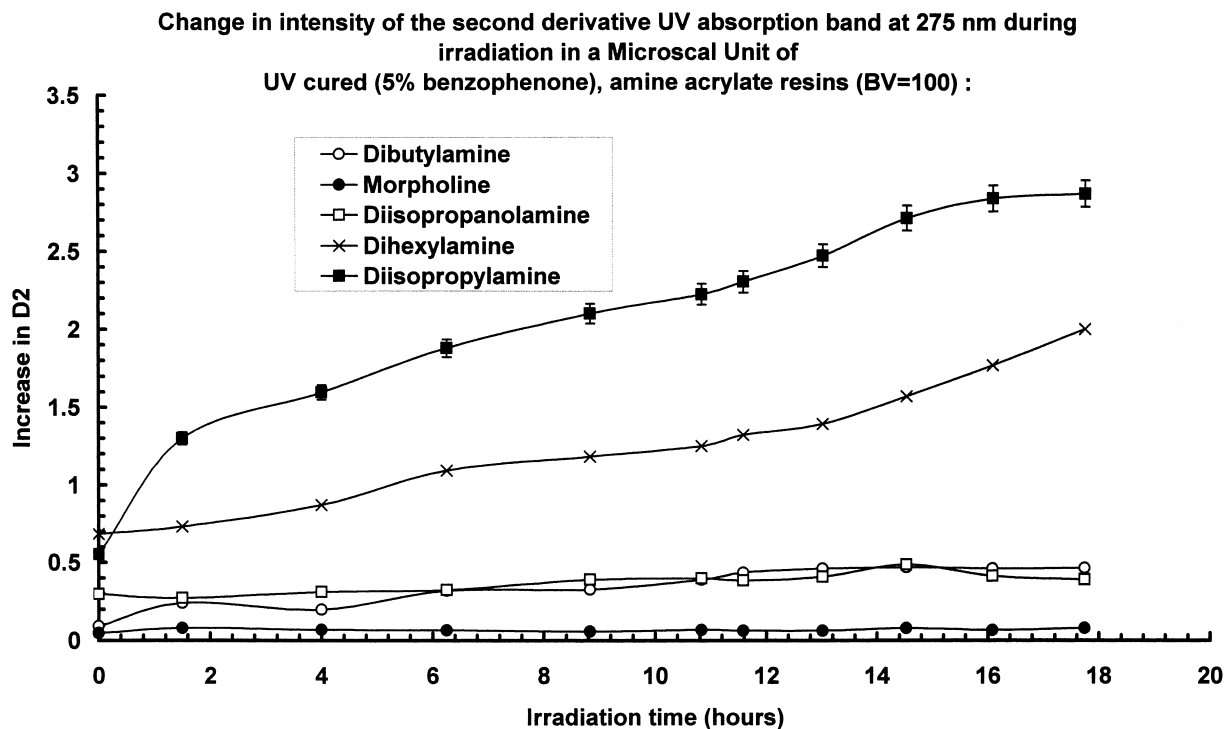


Fig. 21. Second order derivative UV absorption at 275 nm versus irradiation time for (○) dibutylamine, (●) morpholine, (□) diisopropanolamine, (×) dihexylamine, (■) diisopropylamine terminated Actilane 430 resin EB cured (B.V. = 100).

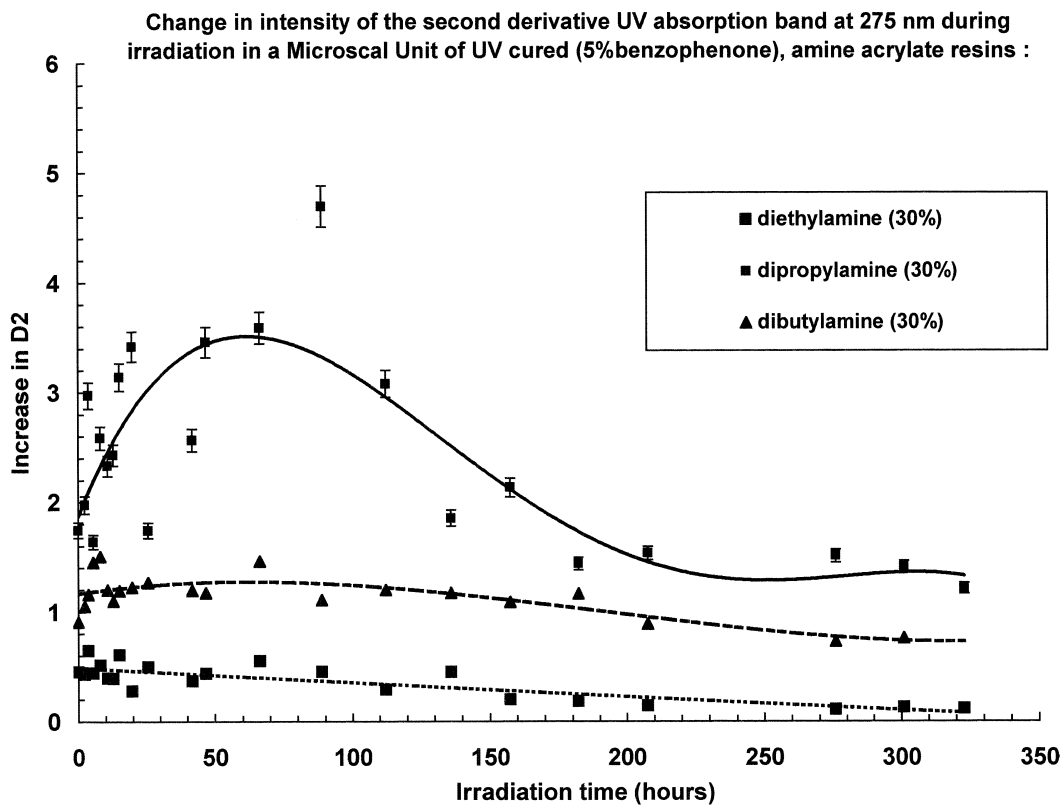


Fig. 22. Second order derivative UV absorption at 275 nm versus irradiation time for (■) diethylamine, (■) dipropylamine and (▲) dibutylamine terminated Actilane 430 resin UV cured (5% w/w benzophenone).

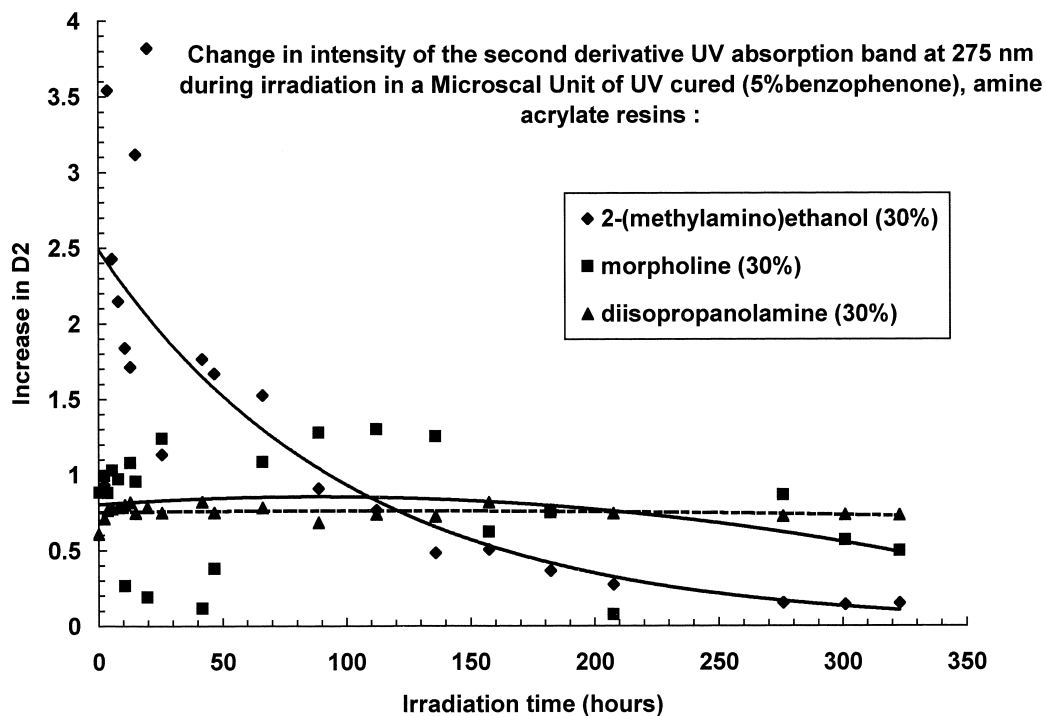


Fig. 23. Second order derivative UV absorption at 275 nm versus irradiation time for (◆) 2-methylaminoethanol, (■) morpholine and (▲) diisopropanolamine terminated Actilane 430 resin UV cured (5% w/w benzophenone).

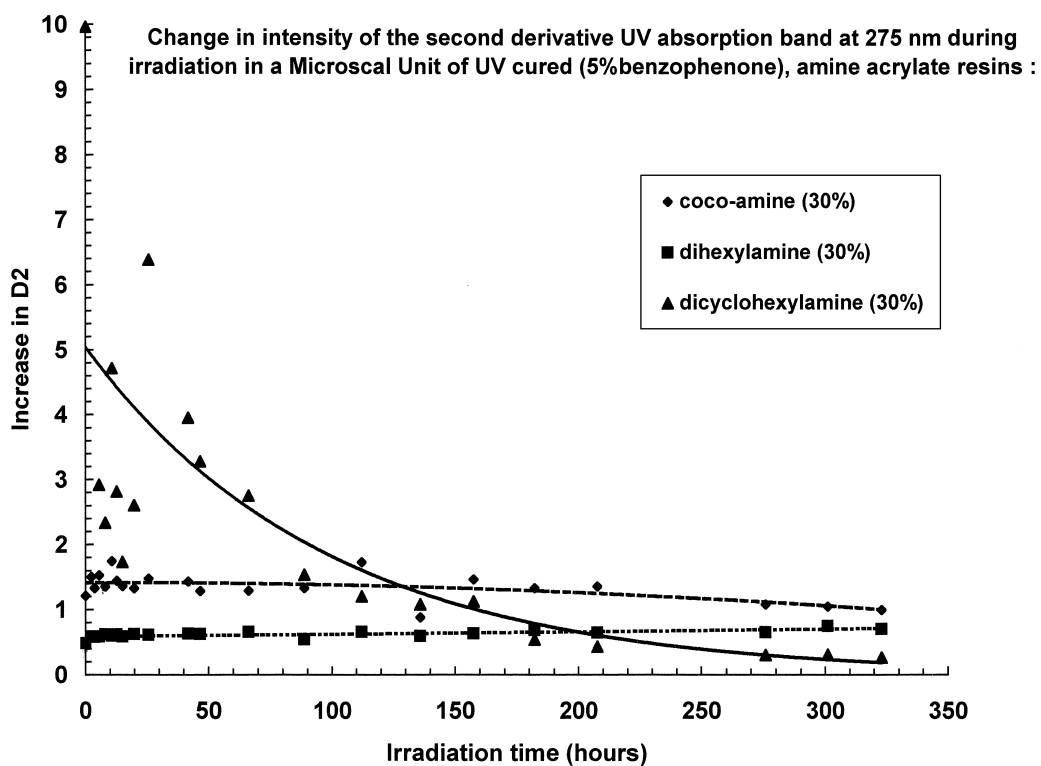


Fig. 24. Second order derivative UV absorption at 275 nm versus irradiation time for (◆) cocoamine, (■) dihexylamine and (▲) dicyclohexylamine terminated Actilane 430 resin UV cured (5% w/w benzophenone).

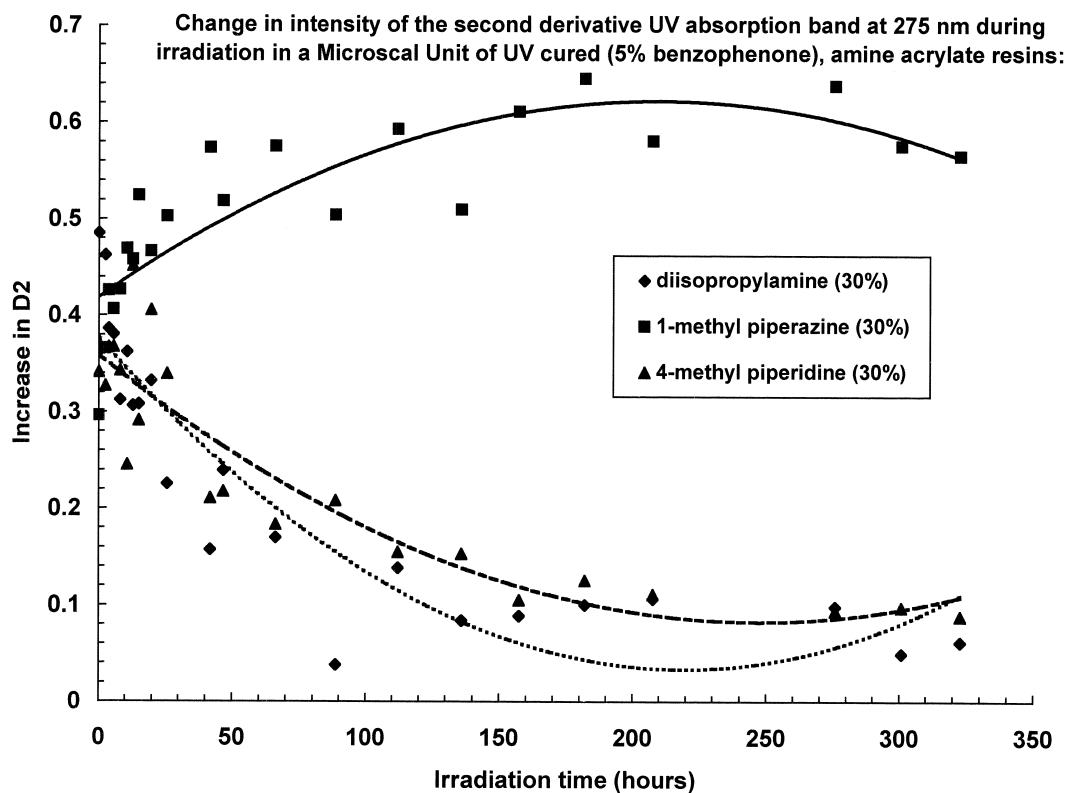


Fig. 25. Second order derivative UV absorption at 275 nm versus irradiation time for (◆) diisopropylamine, (■) 1-methylpiperazine and (▲) 4-methylpiperidine terminated Actilane 430 resin UV cured (5% w/w benzophenone).

The UV cured coatings were examined at a BV = 100 and data compared in Figs. 20 and 21. In this study a selection of amine acrylates are shown irradiated over a period of 400–500 h (Fig. 20) while others are shown over a period of 20 h only. The rapid initial rate of hydroperoxide formation is quite crucial in the mechanism. In many cases UV cured systems undergo greater increases in UV absorption than their EB counterparts. The photosensitising effect of the residual photoinitiator plays an important role here and as seen from the data (Fig. 20) induces an initial rapid rise in UV absorption followed by a marked decrease and then a long plateau effect (as of the OH in some cases). The dialkylamines are again more susceptible to oxidation and UV change than the alkanolamine and the dicyclohexylamine. The resin with 4-methylpiperazine also exhibits a low profile. The rapid initial increase is marked for both the dialkylamines (diisopropylamine and dihexylamine). The dibutylamine also exhibits a small gradual increase. However, the diisopropanolamine resin exhibits no change in UV absorption. The morpholine coating also exhibits a low profile.

UV cured coatings were also examined with a total amine content of 30% w/w for comparative interest. The data are compared in Figs. 22–25 for all of the amine systems. Firstly, significantly larger increases in

UV absorption generation are observed as may be expected from the higher amine content.

4. Conclusions

A number of dialkylamine-terminated diacrylate resins have been prepared by a Michael addition reaction of a secondary amine with a triacrylate diluent monomer. Photocuring rates are found to be dependent upon the extent of UV absorption of the photoinitiator used with ITX in this case exhibiting the most rapid cure. This was followed by Darocur 1173 and the lowest rate with benzophenone. There was no consistency in cure rate with amine structure. Transient absorption spectra on conventional microsecond flash photolysis are assigned to the formation of free radical intermediates formed by electron transfer. Photoinduced polymerisation activities of the resins as measured by real-time infrared spectroscopy were found to be closely related to the formation of such transient species. The initiator structure is the more determining factor.

The photo-oxidative stability and photoyellowing (by UV derivative absorption) of the cured coatings were studied after both UV and electron-beam curing through Fourier transform infra-red (FTIR) and second derivative UV spectroscopic methods and hydroper-

oxide analysis. On photooxidation UV cured diluent monomer was found to undergo oxidation at a higher rate than EB cured systems. Initial photooxidation of the coatings as measured by hydroperoxide analysis and hydroxyl index via FTIR analysis exhibited similar changes. Again the oxidation profiles are dependent upon the terminal amine structure with 1-methylpiperazine exhibiting the strongest oxidation. Hydroxyl index showed generally an initial rise followed by a sharp decline and then a slow increase over much longer irradiation periods. The presence of the amine functionality is found to be an effective scavenger of oxygen and hydroperoxide formation in EB cured coatings. In the UV cured coatings the hydroperoxide levels were found generally to be significantly higher than in EB systems due to the photosensitising effect of the residual photoinitiator. Diluent monomer terminated with dialkylamine groups are found to be more prone to oxidation and UV absorption increase (yellowing) than alkanolamines followed by cycloaliphatic amines and heterocyclic amines. UV cured resins exhibit a more facile transient photoyellowing than the same electron-beam cured systems, and this is associated with hydrogen-atom abstraction and oxidation of the alkylamine group by the residual photoinitiator enhancing the rate of hydroperoxidation of the amine group.

Acknowledgements

The authors thank Akcros Chemicals, Eccles, Manchester, UK for financial support of this programme of work for one of them (M.M.).

References

- [1] Allen NS, Robinson PJ. *J Photochem Photobiol, A: Chemistry* 1989;47:223–47.
- [2] Segurola J, Allen NS, Edge M, McMahon A, Wilson S. *Polym Degrad Stab* 1999;64:39–48.
- [3] Gismondi TE. *J Radiation Curing* 1984;11(2):14.
- [4] O'Hara KO. Society of Manufacturing Engineers. Technical Paper FC85-421, 1985.
- [5] Hara KO. *Polymers Paint Colour J* 1981;171:11.
- [6] Schmid SR. *J Radiation Curing* 1984;11(2):19.
- [7] Decker C, Bendaikha T. *Polym Prepr* 1984;25(1):42.
- [8] Allen NS, Robinson PJ, White NJ, Skelhorne GG. *Eur Polym J* 1984;20:13–18.
- [9] Allen NS, Robinson PJ, White NJ, Skelhorne GG. *Eur Polym J* 1985;21:97–102.
- [10] Allen NS, Robinson PJ, White NJ, Skelhorne GC. *Eur Polym J* 1987;19:147–60.
- [11] Allen NS, Robinson PJ, White NJ, Clancy R. *Polym Degrad Stab* 1989;21:245–55.
- [12] Allen NS, Robinson PJ, White NJ, Clancy R. *Eur Polym J* 1989;25:145–8.
- [13] Allen, NS, Robinson, PJ, White, NJ, Clancy, R. *Am Chem Soc Div Polym Chem Symp Sers (Dallas)* April 1990;417:346–62.
- [14] Allen NS, Lo CK, Salim MS, Jennings P. *Polym Degrad Stab* 1990;28:105–14.
- [15] Allen NS, Lo C.K. Salim, M.S. Applications and properties of amine synergists in UV and EB curable coatings. Radtech "Europe" 89, Florence 9–11 October 1989, p. 253.
- [16] Allen NS, Catalina F, Green PN, Green WA. *Eur Polym J* 1985;21:847.
- [17] Allen NS, Mallon D, Catalina F, Timms AW, Green WA. *Eur Polym J* 1992;28:647.
- [18] McKellar JF, Allen NS. *Photochemistry of man made polymers*. Oxford: Elsevier Applied Science, 1979.